ABSTRACT

Title of Dissertation: On Lifetime Maximization and
Fault Tolerance Measurement
in Wireless Ad Hoc and Sensor Networks

Fangting Sun, Doctor of Philosophy, 2007

Dissertation directed by: Professor Mark A. Shayman
Department of Electrical and Computer Engineering

In this dissertation we study two important issues in wireless ad hoc and sensor networks: lifetime maximization and fault tolerance. The first part of the dissertation investigates how to maximally extend the lifetime of randomly deployed wireless sensor networks under limited resource constraint, and the second part of the dissertation focuses on how to measure the fault tolerance and attack resilience of wireless ad hoc networks.

When trying to maximize the lifetime of randomly deployed wireless sensor networks, we take the approach of adaptive traffic distribution and power control. After abstracting the network into multiple layers, we can model the lifetime maximization problem as a linear program. First we focus on the scenario where transmission energy consumption plays the dominant role in overall energy consumption, that is, the receiving and processing energy consumption is ignored. In

this case we mathematically prove that in order to maximally extend the network lifetime, each node should split its traffic into two portions, where one portion is sent directly to the sink, and the other one to its neighbor in the next inner layer. Next we consider the effect of incorporating the processing energy consumption. In this case, we have a similar observation: for each packet to be sent, the sender should either transmit it using the transmission range with the highest energy efficiency per bit per meter, or transmit it directly to the sink. This is also proved true under some general conditions. Besides studying the upper bound of maximum achievable lifetime extension, we discuss some practical issues, such as how to handle the signal interference caused by adaptive power control. Finally, we propose a fully distributed algorithm to adaptively split traffic and adjust transmission power for randomly deployed wireless sensor networks. Extensive simulation studies demonstrate that the network lifetime can be dramatically extended by applying the proposed approach in various scenarios.

Besides studying the lifetime extension problem for fully deployed wireless sensor networks, in this dissertation we also investigate how to extend the network lifetime via joint relay node deployment and adaptive traffic distribution. We considered wireless sensor networks with two types of nodes: sensors and relays. Sensor nodes will be deployed randomly under certain coverage constraint, and relay nodes will be deployed in a partially controlled way such that the network lifetime can be maximally extended. We formulated the joint relay deployment and adaptive traffic distribution problem as a mixed-integer nonlinear program problem. Since this problem is NP-hard in general, we propose a greedy heuristic to attack it. The numerical results demonstrate that significant network lifetime extension can be achieved if relay nodes can be deployed in an effective way. For

example, when the proposed joint scheme is used, adding 10% extra relay nodes can extend the network lifetime by 50% further compared to using adaptive traffic distribution and power control solely for a large scale sensor network with 2000 nodes. We then conduct a set of simulations to verify the numerical results. Since some approximations have been made when solving the problem numerically, lifetime extension obtained by the numerical solution is slightly higher than the network lifetime extension obtained in the simulation. However, the network lifetime extension is still significant.

In the second part of this dissertation, we investigate how to measure the fault tolerance and attack resilience for randomly deployed wireless ad hoc networks. Due to the randomness and distributiveness of such networks, traditional measurement metrics, such as network connectivity, may not work well. Before proposing the metric for fault tolerance and attack resilience measurement, we first propose two new metrics to measure the average case of network service quality: *average pairwise connectivity* and *pairwise connected ratio*, where the former denotes the average number of node-disjoint paths per node pair in a network and the latter is the fraction of node pairs that are pairwise connected. We derive a theoretical upper-bound for the average pairwise connectivity of randomly deployed wireless ad hoc networks, which can approximate the exact value very well. Based on these two metrics, we then propose the fault tolerance and attack resilience metric: α-p-*resilience*, where a network is α-p-resilient if at least α portion of nodes pairs remain connected as long as no more than p fraction of nodes are removed from the network. The fault tolerance and attack resilience of randomly deployed wireless ad hoc networks are then studied under different attack models.

On Lifetime Maximization and Fault Tolerance Measurement in Wireless Ad Hoc and Sensor Networks

by

Fangting Sun

Dissertation submitted to the Faculty of the Graduate School of the
University of Maryland, College Park in partial fulfillment
of the requirements for the degree of
Doctor of Philosophy
2007

Advisory Committee:

Professor Mark A. Shayman, Chairman
Professor Armand Makowski
Professor Richard J. La
Professor Sennur Ulukus
Professor Guangming Zhang

DEDICATION

To my parents.

ACKNOWLEDGEMENTS

First of all, I would like to express my gratitude to my advisor, professor Mark A. Shayman, who has placed his confidence on me during my Ph.D. studies. During these years, he has put so many efforts to help me find good directions and conduct high quality research. I also value his influences for my vision, attitude, energy, and desire of my professional and personal developments. Meanwhile I would like to thank professor Makowski for his help on the fault tolerance problem.

I would like to thank professor La, professor Ulukus, and professor Zhang for serving in my committee. I would like to thank Dr. Medhi Kalantari, Dr. Abishek Kashyap, Dr. Tuna Guven and Anuj Rawat, for invaluable cooperations and discussion during the last five years. I would also like to thank all the friends throughout University of Maryland for giving me such happy years.

Meanwhile, I am also grateful to my parents for their love and unconditional support. They have made countless efforts to let me have better education chances and make sure that I can explore my future according to my dreams. As a consequence, all my accomplishments are also their accomplishments.

Finally, no happiness of achievement can be completed without sharing with my husband and my lovely son.

TABLE OF CONTENTS

LIST OF TABLES

LIST OF FIGURES

Chapter 1

Motivation and Contributions

During the last decade, wireless ad hoc and sensor networks have become a very active research area. Roughly speaking, a wireless ad hoc network is a group of nodes without requiring centralized administration or fixed network infrastructure, in which nodes can communicate with other nodes out of their direct transmission ranges by cooperatively forwarding packets for each other [47, 60]. Since wireless ad hoc networks can be easily and inexpensively set up as needed, a wide range of applications have been envisioned, such as search and rescue, disaster relief, target tracking, and smart environments. However, before ad hoc networks can be widely used in practice, there still remain a lot of important issues to be solved. In this dissertation, we will study two important issues: network lifetime maximization in wireless sensor networks, and fault tolerance and attack resilience measurement in wireless ad hoc networks.

1.1 Lifetime Maximization in Wireless Sensor Networks

Wireless sensor network, a special type of wireless ad hoc network, has drawn extensively attentions due to the demand of future combat systems and plenty of civilian applications, such as battlefield surveillance, environment and habitat monitoring, healthcare applications, home automation, and traffic control [1, 12, 23, 39, 40, 48, 61, 65]. A wireless sensor network usually consists of spatially distributed autonomous devices using sensors to cooperatively monitor physical or environmental conditions at different locations. In addition to one or more sensors, each node in a wireless sensor network is typically equipped with a wireless communications device, a small microcontroller, and an energy source, usually a battery.

In many applications, wireless sensor networks are deployed in a very large scale. To make such deployment affordable and viable, sensors are usually made small and cheap. Therefore the amount of energy each node can carry is also very limited. Meanwhile, replacing batteries in those sensor nodes will be either difficult or extremely costly. This makes energy become one of the most precious resources in wireless sensor networks. This also motivates us to study how to efficiently utilize the limited energy such that lifetime of such networks can be maximized[1].

In the literature, lifetime maximization in wireless ad hoc and sensor networks is a very active research topic and various approaches have been proposed. Below are some of them that are related to our work.

[1]In the literature, various definitions of network lifetime have been proposed. Roughly speaking, a network is regarded as alive if it still can operate properly, such as no nodes have become dead.

- *Energy aware routing*: In traditional routing protocols designed without considering the energy constraint, some nodes may die much faster than other nodes due to extra packet forwarding burden. To address this issue, some researchers have proposed energy aware routing [8, 13, 28, 52–54]. For example, in [13], the authors study how to design energy aware routing protocols for ad hoc networks where the nodes have limited initial amounts of energy and each node may adjust its power within a certain range that determines the set of possible one hop away neighbors. The authors propose algorithms to select the routes and the corresponding power levels such that the time until the batteries of the nodes drain-out is maximized, and show that in order to maximize the lifetime, the traffic should be routed such that the energy consumption is balanced among the nodes in proportion to their energy reserves. One big assumption in [13] is that the topology of network needs to be known, which limits its applicability.

- *Energy-aware sleeping scheduling and medium access control*: Another approach to extend the lifetime of wireless ad hoc sensor network is to design energy aware sleep scheduling and Medium Access Control (MAC) protocols, such as [11, 51, 66]. By taking into the consideration that nodes in wireless sensor networks are inactive and/or idle in most time, scheduling and MAC protocols can be designed in a more energy efficient way. Their results also demonstrate that significant lifetime extension can be achieved when such approaches are used.

- *In-network data aggregation*: By applying in-network data aggregation, the network lifetime may also be significantly extended, as demonstrated in [29, 32, 42]. In sensor networks, the data collected by sensors in the nearby

neighborhood are usually correlated. If the redundancy among the collected data can be exploited, less traffic is needed to be forwarded, which can reduce the forwarding burden of those bottleneck nodes and may consequently extend the network lifetime.

- *Energy-efficient clustering and hierarchical routing*: This approach tries to divide the network into multiple clusters and routing in a hierarchical structure, as demonstrated in [3, 12, 24, 67]. For example, in [3], a distributed randomized clustering algorithm is proposed to organize the sensors in a wireless sensor network into clusters, and observe that the energy saving increasing with the number of levels in the hierarchy. If clustering can be done in an efficient way, the network lifetime can also be extended.

- *Joint mobility and Routing for Lifetime Elongation*: If the data sink is allowed to move around when collecting data, then routing and mobility control can be jointly considered to further extend the network lifetime, as demonstrated in [38]. In their work, the authors try to design optimal data collection protocols by taking both base station mobility and multi-hop routing into consideration. Their results have shown that significant lifetime extension can be achieved. However, one major disadvantage of their approach is that in reality seldom data sink can be mobile.

- *Energy-aware resource allocation*: Another straightforward way to extend the network lifetime is to allocate more resources into specific areas to relieve the bottleneck effect, as illustrated in [27, 33, 64].

- *Energy-balanced data propagation*: Another promising solution to extend the network lifetime is energy-balanced data propagation, as demonstrated in

[20, 34, 49, 63]. In [20, 34, 49], Rolim et. al. try to derive schemes which can make all nodes in network die at the same time by focusing on a special strategy, where for each node, when it has a packet to send, it only has two options: either send to its immediate down stream relay, or directly send to the sink. They later derive an algorithm and proved that it can compute the traffic split ratio optimally so that all nodes will die at the same time. In [63], the authors also experimentally study energy-balanced data propagation by taking into consideration the processing energy consumption with the goal to be let nodes consume energy at same speed.

In this dissertation the problem of extending network lifetime is attacked by applying adaptive traffic distribution and power control. The basic idea is to let each sensor adaptively split its traffic with each portion being transmitted using a different transmission range such that the network lifetime can be maximized. This is motivated by the following observation: in a sensor network where nodes need to send data to the sink and all nodes use the same transmission power, nodes around the sink will experience much higher power consumption rate than faraway nodes because of the extra relaying burden. As a consequence, the nodes around the sink will run out of energy pretty fast, resulting in the quick death of the network, though there is still considerable unused energy left in those nodes far away from the sink. If nodes can adaptively adjust their transmission ranges, nodes far away from the sink can at least directly send data to the sink to reduce the relaying burden of the nodes around the sinks, and consequently increase the network lifetime.

After abstracting the network using a layered model, we model the lifetime maximizing adaptive traffic distribution and power control problem as a linear pro-

gram. In order to help better understand the problem and meanwhile shed light on the solution to more complicated scenarios, we first study the scenario by ignoring the processing energy consumption (e.g., circuit-level energy consumed during transmission and receiving). In this case, both numerical results and theoretical analysis have confirmed the following important finding: in order to maximally extend the network lifetime, for each packet to be sent, the node should transmit it either directly to the sink, or to the immediate next inner hop. The significance of such a finding lies in the fact that it can lead to very simple and efficient distributed algorithms for splitting the traffic and adjusting the transmission power adaptively.

We then study the effect of incorporating processing energy consumption into our model. In this case a similar finding is obtained: for each packet to be sent, the sender should transmit it either directly to the sink, or to the certain inner layers with the highest energy efficiency per bit per meter. Moreover, the results indicate that incorporating processing energy consumption will not decrease the effectiveness of the proposed adaptive traffic distribution and power control approach. Furthermore, incorporating the processing energy consumption can even make the maximally extensible network lifetime increase. The results also show that the variation of the processing energy consumption will not significantly affect the extensible lifetime. In other words, the proposed approach can work in various scenarios under various sensor node settings.

Although adaptive transmission power adjustment can lead to significant lifetime extension, in practice, we may not be able to reach the maximally achievable extension that it has promised. One reason is that such an adaptive transmission power adjustment scheme can introduce extra signal interference, especially when

long transmission ranges are used. To combat this issue, instead of focusing on designing complicated scheduling and medium access control schemes, in this work we propose a very simple yet effective approach: limiting the number of nodes that are allowed to adjust their transmission range. Specifically, only a certain number of nodes nearest to the sink are allowed to perform adaptive transmission range adjustment, and all other nodes will keep their transmission power fixed. Although this may reduce the maximally achievable lifetime extension, the simulation results demonstrate that the lifetime extension is still significant.

Decentralization is one key feature of wireless sensor networks. In order to make the proposed approach practically applicable, we need to implement it in a fully distributed way. Towards this goal, we propose Energy-Aware Data Propagation Algorithm, a fully distributed algorithm, to perform online adaptive traffic distribution and transmission range adjustment. Our extensive results demonstrate that the algorithm is very efficient and can significantly extend the lifetime of randomly deployed wireless sensor networks in various scenarios and network settings. This work can also be found at [56, 57].

In the above lifetime maximizing adaptive traffic distribution and transmission power adjustment problem, we have focused on the situation in which the optimization is performed after the network has been completely deployed, and have implicitly assumed that certain quality of service (QoS) requirements, such as network coverage constraint[2], have been taken into consideration during the deployment. In addition to that, in this work we have also studied the situations that there are two types of nodes in a wireless sensor network: sensor nodes and

[2]Roughly speaking, we say a certain point has been covered if this point lies in at least one active sensor node's coverage range.

relay nodes. Sensor nodes are randomly deployed with certain network coverage requirement, and relay nodes will be deployed in a partially controlled way to further extend the network lifetime. We have investigated how to extend the network lifetime via joint optimization of node deployment and adaptive traffic distribution. Since this optimization problem is mixed integer nonlinear programming problem, which is NP-hard, we proposed a greedy algorithm to attack it. The numerical results show that significant gain can be achieved, which has also been confirmed by the simulation studied. This work can be found at [58].

1.2 Fault Tolerance and Attack Resilience Measurement of Wireless Ad Hoc Networks

In addition to lifetime maximization with energy constraint, fault tolerance and attack resilience are also important issues in wireless ad hoc and sensor networks. In wireless ad hoc networks, due to the fragile wireless connections and possible mobility, link breakages may happen very frequently. Meanwhile, some nodes may be removed from the network due to the exhaustion of battery power. Therefore, the study of fault tolerance should be an indispensable component, where the network fault tolerance denotes the ability of a network to continue operating even though some of its components have malfunctioned or failed[3]. Furthermore, such networks may also be deployed in adversarial environments, and some parts of the network may become unusable due to the attacks from malicious parties. For example,

[3]In this chapter "fault" refers to those link or node removals caused unintentionally, that is, no malicious parties are involved. Those link or node removals involving malicious parties will be referred to as "attack".

in wireless sensor networks, due to lacking enough physical protection, nodes can be easily captured, compromised, or hijacked. Since nodes in such networks usually share the common communication channels, malicious parties can also launch jamming attacks to disrupt the normal communications, which can consequently result in some nodes or links becoming disconnected from the network. In such circumstances, the ability of a network to continue operating even under attacks becomes critical, which is referred to as *attack resilience*. Before further studying the fault tolerance and attack resilience of a wireless ad hoc network, we need to know how to quantify them. Without a metric, we cannot say one network is more fault tolerant or attack resilient than another network.

To measure the network fault tolerance, one widely used metric is network connectivity. For example, network fault tolerance has been defined as the maximum number of elements that can fail without inducing a possible disconnection in the network [43, 50], that is, the network connectivity [6]. However, the use of network connectivity to measure network fault tolerance only focuses on the worst case. First, a network not being k-connected only implies that there exists some choice of $k-1$ nodes whose removal would disconnect the network, but does not mean that if $k-1$ nodes are removed, it is likely that the network will be disconnected. Second, even if the removal of a group of nodes disconnects the network, it is still possible that only one or a small number of nodes become isolated from the rest, and may not have a significant impact on the usefulness of the network, and the network may have high average pairwise connectivity and pairwise connected ratio.

Recently, the attack resilience issues have also drawn extensive attention. [2] first study the attack resilience issues in scale-free networks. Following this, the attack resilience of some other networks have been studied, such as Internet [10, 15,

16], food web [18, 19], protein network [30], email network [45], complex network [25], and so on. To measure the attack resilience, one candidate is the average vertex-to-vertex distance as a function of the number of vertices removed [2], or equivalently, the average inverse geodesic length [25], where both measure the average distance between node pairs in a network. However, such a metric may not be appropriate to measure the attack resilience of wireless ad hoc networks for the reason that in such networks the average vertex-to-vertex distance will increase with the increase of network size for a fixed node density, while it is not necessarily accompanied by a decrease in the network attack resilience.

To overcome the limitation of the existing metrics to measure the fault tolerance and attack resilience of wireless ad hoc networks, we first propose two new metrics to measure the average case of network service quality: *average pairwise connectivity* and *pairwise connected ratio*, where the former denotes the average number of node-disjoint paths per node pair in a network and the latter is the fraction of node pairs that are pairwise connected. We also derive a theoretical upper-bound for the average pairwise connectivity of randomly deployed wireless ad hoc networks, which can approximate the exact value very well. Based on these two metrics, we then propose the fault tolerance and attack resilience metric: α-p-*resilience*. Specifically, a network being α-p-resilient means that its expected pairwise connected ratio is no less than α as long as no more than p fraction of nodes are removed. It is worth pointing out that the α-p-resilience of a network may not be the same under different node removal patterns. For example, a network is usually more α-p-resilient to random fault than to attack. A similar metric can be used to measure the decrease of average pairwise connectivity under fault or attack.

Under the proposed metric, we also study the fault tolerance and attack resilience of wireless ad hoc networks under different node failure patterns: random node removal, selective node removal, and partition attack. Experimental studies demonstrate that when the node density is relatively high, wireless ad hoc networks are more sensitive to partition attacks than selective node removal attacks and random node failures, and selective node removal attacks are a little bit more damaging than random node removal; when the node density is extremely low, all the three node removal methods have similar effects, with partition attacks and selective node removal attacks being a little bit more damaging than random node removal. This work can be found at [59].

1.3 Thesis Organization

The rest of this dissertation is organized as follows. Chapter 2, Chapter 3 and Chapter 4 study how to maximally extend the lifetime of wireless sensor networks under energy constraint. Specifically, Chapter 2 focuses on a simplified scenario where processing and receiving energy are ignored. Chapter 3 studies the effect of incorporating the processing energy consumption and describes a fully distributed algorithm to perform online adaptive traffic distribution and transmission range adjustment. Chapter 4 investigates how to maximize the network lifetime via joint optimization of node deployment and adaptive traffic distribution. The service availability, fault tolerance and attack resilience measurement of wireless ad hoc networks is studied in Chapter 5. Finally, Chapter 6 concludes this dissertation and presents future directions.

Chapter 2

Wireless Sensor Network Lifetime Maximization Without Considering Receiving & Processing Power

As mentioned in Chapter 1, in our work we attack the problem of extending network lifetime by applying adaptive traffic distribution and transmission range adjustment. The basic idea is to let each node adaptively split its traffic with each portion being transmitted using a different transmission range such that the network lifetime can be maximized. As suggested in [13], we define the *network lifetime* as the time elapsing between network deployment and the moment when the first node dies.

To help better understand lifetime maximizing adaptive traffic distribution and power adjustment problem and shed light on the solutions to more complicated scenarios, we first study the lifetime maximization problem by ignoring process-

ing and receiving energy consumption. This applies to the situations where the transmitting power plays a dominant role, such as in long range communication. The rest of this chapter is organized as follows. Section 2.1 describes the network model and the problem formulation. Section 2.2 presents the numerical results. The theoretical analysis is presented in Section 2.3. Finally Section 2.4 summarizes this chapter.

2.1 System Model and Problem Formulation

We consider randomly deployed wireless sensor networks consisting of a set of homogeneous wireless sensors. Each sensor needs to submit the collected information to the sink which is roughly located at the center of the area. We assume that all sensors have the same amount of initial energy, denoted by E. This is usually true in randomly deployed wireless sensor networks. However, we do not put an energy constraint on the sink, which also makes sense in practice. Given the network to be deployed, some Quality of Service (QoS) requirements, and specific types of sensors, we also pose a minimum and maximum transmission range limitation for each sensor, denoted by r_{min} and r_{max}. The value of r_{min} can be determined by both hardware limitation and QoS requirements, such as network connectivity. The value of r_{max} is usually decided by hardware constraint. Currently the maximum transmission range in general sensor networks is around several hundred meters, however, along with the advance of the technology, especially the increase of the receiver sensitivity, the maximum transmission range for sensors will be much longer [37].

In this work, similar to [27,62], we model the transmission energy consumption

at each node as follows:

$$P_t(r) = \beta \cdot r^{\alpha} \quad \text{per bit.} \tag{2.1}$$

Here α is the path loss exponent, r is the targeted transmission range, and β is a scalar indicating the energy needed to successfully convey an information bit to a unit distance. Generally, the traffic load in sensor network is low, so in this work we do not consider MAC protocol and assume perfect MAC protocol is available.

Next we model the lifetime maximization problem. If the exact distances between all pairs of nodes are known, it is possible to model the problem precisely. However, in randomly deployed wireless sensor networks, such information is usually impossible to obtain. To make the problem tractable, we further abstract the network model by assuming that the sensors are (deterministically) uniformly deployed. These assumptions will be relaxed later when we conduct performance evaluation. We then divide the network into multiple layers: a node belongs to the l^{th} layer if and only if its distance to the sink lies in the range $((l-1) \cdot r_{min}, l \cdot r_{min}]$, and the layer 0 is the sink. Thus, the width of each layer is taken to be r_{min}.

We first begin with a simple one-dimensional case, where the sensors are equally spaced deployed along a line with the sink located at the center of line. Let L denote the total number of layers. For any integers l, k with $0 \leq k < l \leq L$, let $x_{l,k}$ denote the average number of bits that a node in the l^{th} layer needs to request nodes in the k^{th} layer to forward per unit time. Let T_{life} denote the network lifetime and $P = \frac{E}{T_{life}}$ be the average energy consumption rate. Here maximizing T_{life} is equivalent to minimizing P. Then we can model the lifetime maximization

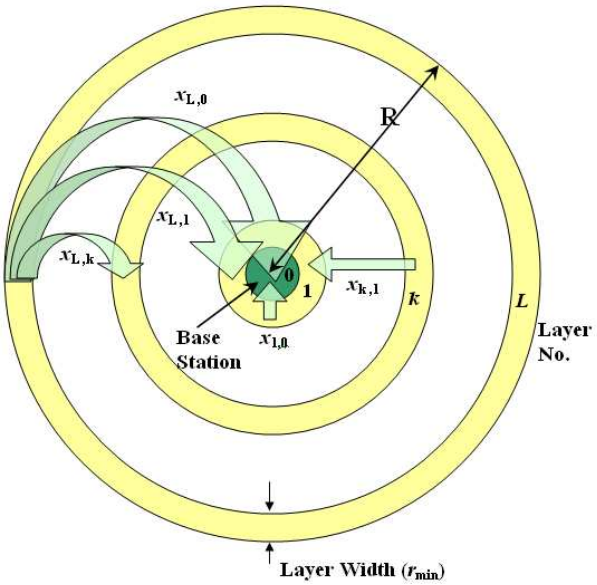

Figure 2.1: Layered network model illustration

problem as the following MIN-MAX linear program:

$$\min_{\{x_{l,k},\ 1\le l\le L,\ 0\le k\le L\}} P \qquad s.t. \tag{2.2}$$

$$\sum_{k=l+1}^{L} x_{k,l} + g = \sum_{k=0}^{l-1} x_{l,k}, \quad 1 \le l \le L \tag{2.3}$$

$$\sum_{k=0}^{l-1} x_{l,k} \times P_{l,k}^{t} \le P, \qquad 1 \le l \le L \tag{2.4}$$

$$x_{l,k} \ge 0, \qquad 1 \le l \le L, \quad 0 \le k < l \tag{2.5}$$

$$x_{l,k} = 0, \qquad (l-k)r_{min} > r_{max}, 0 \le l, k \le L \tag{2.6}$$

$$x_{l,k} = 0, \qquad 0 \le l \le k \le L \tag{2.7}$$

where $P_{l,k}^{t} = P_t((l-k)r_{min})$. Here condition (2.3) is for traffic conservation, that is, the amount of transmitted traffic should be equal to the amount of received plus generated traffic. Condition (2.4) indicates that the energy consumption rate of all nodes should be no more than P, where the node with the maximum energy consumption rate will determine the network lifetime. Condition (2.5) is introduced to guarantee that the solutions are feasible. Condition (2.6) limits each node's

maximum transmission range. Condition (2.7) prevents nodes from sending traffic further away from the sink.

Next we study the more general two-dimensional situation. The network model is illustrated in Fig. 2.1. Let R denote the radius of the network and let L denote the total number of layers in the network, that is, $L = \lceil \frac{R}{r_{min}} \rceil$. Similarly to one-dimensional case, we define g and $x_{l,k}$ for two-dimensional case. We can readily check that the ratio between the number of nodes in the k^{th} layer and the number of nodes in the l^{th} layer $(k > l)$ is $\frac{2k-1}{2l-1}$. Thus the average number of bits that a node in the l^{th} layer will receive from nodes in the k^{th} layer $(k > l)$ should be $\frac{2k-1}{2l-1} x_{k,l}$. Then the two dimensional case can be modeled as the following MIN-MAX linear program:

$$\min_{\{x_{l,k},\ 1\le l\le L,\ 0\le k\le L\}} P \qquad s.t. \tag{2.8}$$

$$\sum_{k=l+1}^{L} \frac{2k-1}{2l-1} x_{k,l} + g = \sum_{k=0}^{l-1} x_{l,k}, \quad 1 \le l \le L \tag{2.9}$$

$$\sum_{k=0}^{l-1} x_{l,k} P_t^{l,k} \le P, \qquad 1 \le l \le L \tag{2.10}$$

$$x_{l,k} \ge 0, \qquad 0 \le k < l, \quad 1 \le l \le L \tag{2.11}$$

$$x_{l,k} = 0, \qquad (l-k) r_{min} > r_{max}, 0 \le l, k \le L \tag{2.12}$$

$$x_{l,k} = 0, \qquad 0 \le l \le k \le L \tag{2.13}$$

where $P_t^{l,k} = P_t((l-k) r_{min})$.

2.2 Numerical Results

Before presenting the theoretical results, we first examine the numerical solutions, and compare the lifetime extension under different settings. The baseline approach is as follows: each layer is only allowed to transmit to its next immediate inner layer, that is, $r_{max} = r_{min}$. In the following comparison, *extended lifetime (or lifetime*

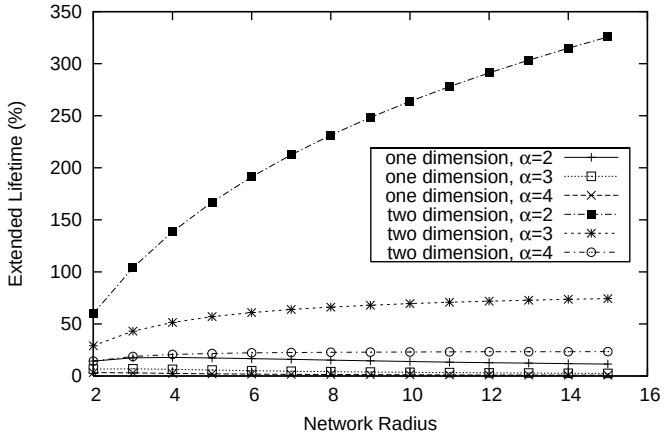

Figure 2.2: Extended lifetime when there is no maximum transmission range constraint for all nodes

extension) denotes the ratio between the extended lifetime by other approach over the lifetime obtained by the baseline approach. In other words, if the extended lifetime is x%, the whole lifetime is (1+x%) times the lifetime of the baseline approach. *network radius* identifies the network size. Without loss of generality we normalize $r_{min} = 1$; then the network with radius R will have R layers.

We first study the maximum possible lifetime extension that can be achieved by applying adaptive traffic distribution and power control. Fig. 2.2 illustrates the numerical results for different network radii and path loss exponents by setting $r_{max} \geq R$ and assuming interference-free medium access scheduling. Fig. 2.2 shows that the adaptive power control scheme is more effective for the two-dimensional network than for the one-dimensional network. For the two-dimensional network, the nodes around the sink need to relay more traffic, so they are more critical than their counterpart in the one-dimensional network in terms of energy consumption. Thus, when we smooth the energy consumption rate by adjusting transmission power, we can get more gain in the two-dimensional network. From these results

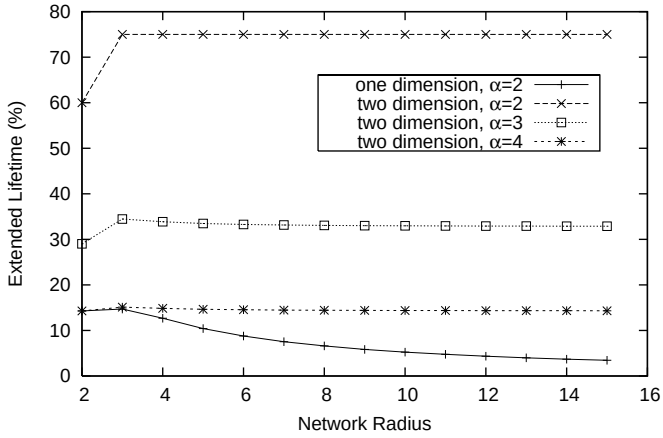

Figure 2.3: Lifetime extension under the constraint $r_{max} = 2r_{min}$

we also observe that the larger the network size, the more the network lifetime can be extended, especially when the path loss exponent is low. When the path loss exponent becomes high, the benefit of increasing transmission range will be reduced due to the fact that longer transmission range results in lower energy efficiency per bit per meter.

Fig. 2.2 also shows that in the two-dimensional network, the network lifetime can be extended about 75% when the path loss exponent is 3, and around 25% when the path loss exponent is 4. When the path loss exponent is 2, the lifetime extension can be up to 325% for the network size 15 (here network size denotes the number of layers in the network).

As we mentioned before, in practice nodes usually have maximum transmission range constraint. So we next study the numerical solutions by imposing maximum transmission range constraint. Fig. 2.3 illustrates the results for one case: $r_{max} = 2r_{min}$. This can be modelled as a linear programming problem by adding constraints $x_{l,k} = 0,\ l - k > 2$ to equations. Similar to Fig. 2.2, Fig. 2.3 shows

that when dimension is higher or the path loss exponent is lower, the network lifetime can be extended more. It also shows that even after imposing such a restrictive constraint, significant lifetime extension can still be achieved: 75%, 33% and 14% for path loss exponent being 2, 3, and 4 respectively for two-dimensional case. Furthermore, given a fixed path loss exponent, the extended network lifetime percentage remains almost the same for different network sizes.

We studied this phenomena a little bit and found following Lemma:

Lemma 2.1 *Let P_1 is the MIN-MAX P for LP 2.8-2.13 with $\alpha = 2, r_{max} = 2r_{min}, L \geq 3$; let P_2 is the MIN-MAX P for LP 2.8-2.13 with $\alpha = 2, r_{max} = r_{min}, L \geq 3$. Then $\frac{P_2}{P_1} \geq \frac{7}{4}$, i.e., the lower bound for the network lifetime extension is 75%.*

Proof:

It is readily to check that when $r_{max} = r_{min}$, the solution for LP 2.8-2.13 is $P_2 = L^2 g P_t(r_{min})$. We then prove this lemma by constructing one feasible solution $\tilde{P}$ for $r_{max} = 2r_{min}$ case.

We slightly modify the original problem by putting one more extra constraint (except $r_{max} = 2r_{min}$): only the inner 3 layers are allowed to adjust their transmission range, while all the other layers keep their transmission range fixed at r_{min},

i.e. $x_{l,k} = 0,\ l > 3, l - k > 1$. Then we can get a simple LP:

$$\min P \quad s.t. \tag{2.14}$$

$$3x_{2,1} + 5x_{3,1} + g = x_{1,0} \tag{2.15}$$

$$\frac{5}{3}x_{3,2} + g = x_{2,0} + x_{2,1} \tag{2.16}$$

$$\frac{7}{5}x_{4,3} + g = x_{3,1} + x_{3,2} \tag{2.17}$$

$$x_{4,3} = \frac{1}{7}(L^2 - 9)g \tag{2.18}$$

$$x_{1,0}P_t(r_{min}) \leq P \tag{2.19}$$

$$4x_{2,0}P_t(r_{min}) + x_{2,1}P_t(r_{min}) \leq P \tag{2.20}$$

$$4x_{3,1}P_t(r_{min}) + x_{3,2}P_t(r_{min}) \leq P \tag{2.21}$$

$\{x_{1,0} = \frac{4}{7}L^2 g, x_{2,0} = \frac{1}{7}L^2 g, x_{2,1} = 0, x_{3,1} = \frac{1}{5}(\frac{4}{7}L^2 - 1)g, x_{3,2} = \frac{3}{5}(\frac{1}{7}L^2 - 1)g\}$ is one set feasible solution to above LP and the corresponding P is $\tilde{P} = \frac{4}{7}L^2 g P_t(r_{min})$. $\tilde{P}$ is one feasible solution to the LP 2.8-2.13 with $r_{max} = 2r_{min}$, then $\tilde{P} \geq P_1$. So $\frac{P_2}{P_1} \geq \frac{7}{4}$. □

Similar to $\alpha = 2$ case, we can prove that when $r_{max} = 2r_{min}$, the lower bound lifetime extension for $\alpha = 3$ is 32.8% when there are more than 4 layers in the network and the lower bound for $\alpha = 4$ is 14% when there are more than 5 layers in network.

The other interesting observation is that the extended lifetime decreases when the network size increases for the one-dimensional case. Through the analysis in the two-dimensional case, we know that when the maximum transmission range is 2, mainly the inner 3 layers count. On the other hand, in the one-dimensional case, the larger the network size, the smaller the relative traffic difference between the inner layers when all nodes use same transmission range. So the gain by adjusting the transmission range is smaller when the network size is larger.

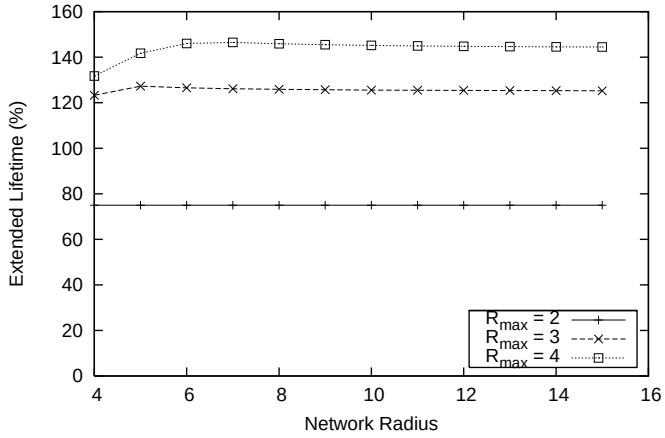

Figure 2.4: Lifetime extension for 2-dimensional case under different r_{max} constraint, $\alpha = 2$

Now we study the more general cases by varying r_{max}. Fig. 2.4 illustrates the numerical results under different r_{max} values, where $\alpha = 2$. We can see that with the increase of r_{max}, the network lifetime extension also increases. This is easy to understand: with the increase of r_{max}, each node has more choices to send traffic to, and the optimization problem becomes less constrained. Similar to the results in Fig. 2.3, we can also observe that the extended lifetime remains almost the same for different network size, 125% for $r_{max} = 3$ and 160% for $r_{max} = 4$. The reason is as before: in this case the network lifetime is mainly determined by how those innermost layers behave.

To demonstrate the important role that the innermost layers play, we consider the following simple strategy obtained by imposing an extra constraint: only those innermost layers that can directly reach the sink are allowed to adaptively adjust their transmission range, while all the other layers fix the transmission range at r_{min}. Fig. 2.5 illustrates the numerical results as well as the comparison to the

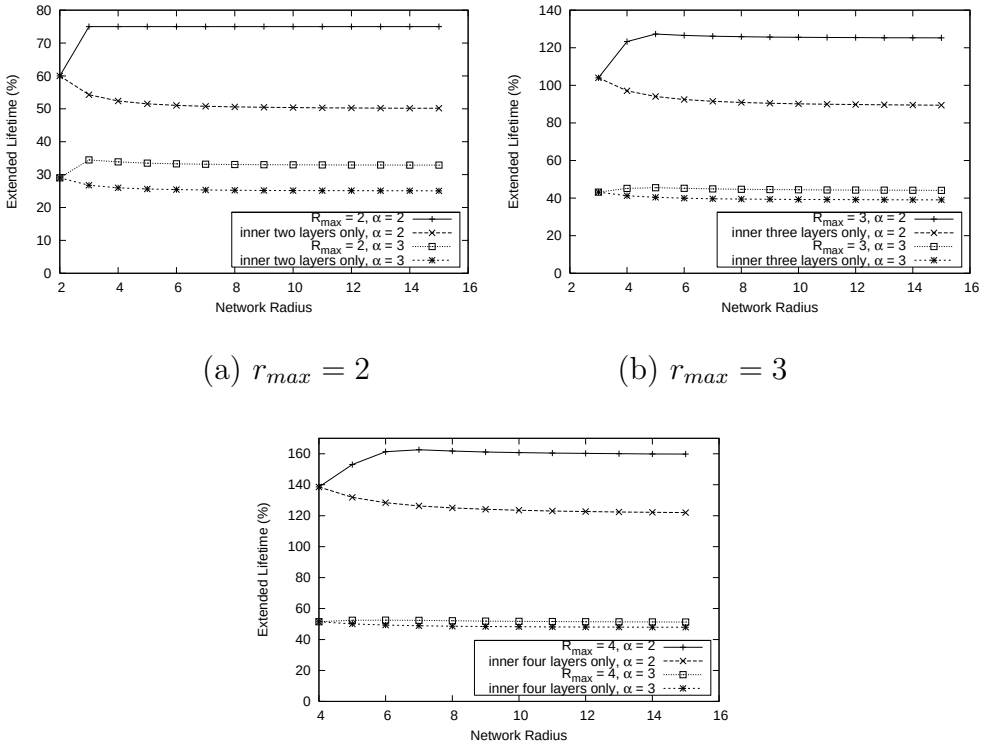

(a) $r_{max} = 2$ (b) $r_{max} = 3$

(c) $r_{max} = 4$

Figure 2.5: Comparison between constraining transmission power adjustment to innermost several layers versus imposing a maximum transmission range constraint.

results without imposing this extra constraint, that is, all nodes can adjust their transmission range up to r_{max}. From these results we can see that although there is performance loss compared to the case where all nodes are allowed to adjust transmission range, the lifetime extension is still significant: 50%, 91% and 126% when only innermost 2, 3, and 4 layers are allowed to adjust their transmission range, respectively. As will be mentioned many times later, the attraction of this extra constraint lies in that it can greatly simplify the implementation: if only some innermost layers are allowed to adjust their transmission power, the scheduling and medium access control protocol can be greatly simplified and the

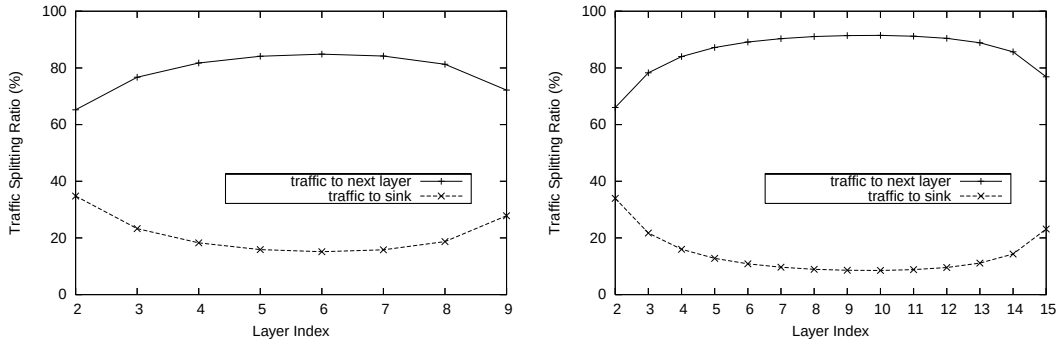

(a) (b)

Figure 2.6: Traffic splitting ratio for each layer. where the whole traffic is split between the next inner layer and the sink. Two-dimensional network with path loss exponent $\alpha = 2$. (a) network radius = 9 (b) network radius = 15

extra signal interference caused by power adjustment can be significantly reduced.

If we take a further look at the numerical solutions to the problem (2.8)-(2.13), we can see for each node its whole traffic will be split into two portions, one is directly sent to the sink and one is sent to the next inner layer, as illustrated in Fig. 2.6. This can be translated into the following statement: when there is no maximum transmission range constraint (e.g., $r_{max} \geq R$), the optimization problem (2.8)-(2.13) should have at least one optimal solution with the following form:

$$\{x_{i,i-1} \geq 0,\ x_{i,0} \geq 0,\ x_{i,j} = 0,\quad 1 \leq i \leq L,\ 1 \leq j \leq i-2\} \tag{2.22}$$

We refer to such a solution as having *standard form*. The attraction of this form lies in that it can direct us to design an efficient and fully distributed algorithm to perform online traffic distribution and power adjustment. We will study this result further in Section 2.3.

From Fig. 2.6, we can see that although the splitting ratio is different, both

subfigures have a similar shape: the nodes in the middle layers will send traffic to sink with a lower ratio, while the nodes in the layers either near the sink or near the boundary will send traffic to the sink with a higher ratio. The reason is that nodes in faraway layers near the boundary have less traffic, so they can afford to send a higher percentage of traffic directly to the sink, and nodes in the innermost layers can afford to send a higher percentage of traffic directly to the sink because their distance to the sink is small.

2.3 Theoretical Analysis

The results in Section 2.2 suggest the following conjecture: when a sensor node can send traffic to the sink directly, then it should either send the traffic to the sink directly, or send to its next inner layer. In this section, we will formally prove this conjecture.

We will give out the detail proof for two-dimensional case and one-dimensional case can be proved similarly.

Theorem 2.2 *When $\alpha > 1$, and each node can reach the sink by adjusting its transmission power, there always exists an optimal solution to the optimization problem (2.8)-(2.13) with the standard form (2.22).*

Proof:

We will show that any optimal solution can be transformed into a solution in standard form (2.22) without losing optimality.

Let $\{x_{i,j}\}$ be an optimal solution. If this optimal solution is not in the standard form, then we can transform $\{x_{i,j}\}$ to $\{\tilde{x}_{i,j}\}$ such that $\{\tilde{x}_{i,j}\}$ is in the standard form. The whole procedure is as follows:

We iteratively apply the following procedure: find the first link $x_{l,l-r} > 0$ ($l \geq 3$) with the following properties:

- $\{x_{i,i-1} \geq 0, x_{i,0} \geq 0, x_{i,j} = 0, 2 < i < l, 1 \leq j \leq i-2\}$, that is, for all $i < l$, except $x_{i,0}$ and $x_{i,i-1}$, no other links can have non-zero traffic value.
- For all $0 < j < l - r$, $x_{l,j} = 0$.

Next we show how to redistribute $x_{l,l-r}$ to the other links. Specifically, we will redistribute the traffic on links in such a way that no traffic will go through the link $(l, l-r)$ and the MIN-MAX power among all layers does not increase. For layer $l - r$, its initial power is:

$$\begin{aligned} P_{l-r} &= (l-r)^\alpha x_{l-r,0} + x_{l-r,l-r-1} \\ &\geq \frac{2l-2r+1}{2l-2r-1} x_{l-r+1,l-r} + \frac{2l-1}{2l-2r-1} x_{l,l-r} + \sum_{i=l+1}^{L} \frac{2i-1}{2l-2r-1} x_{i,l-r} + g \end{aligned} \tag{2.23}$$

where $\frac{2l-2r+1}{2l-2r-1} x_{l-r+1,l-r} + \frac{2l-1}{2l-2r-1} x_{l,l-r} + \sum_{i=l+1}^{L} \frac{2i-1}{2l-2r-1} x_{i,l-r} + g = x_{l-r,0} + x_{l-r,l-r-1}$ is the traffic that layer $l - r$ needs to transmit.

We split traffic $x_{l,l-r}$ into two parts $\Delta x_{l,l-r+1}$ and $\Delta x_{l,0}$ which will be sent to the layer $l - r + 1$ and the sink respectively. To conserve traffic and to keep the layer l power consumption unchanged, we need to have

$$\begin{cases} \Delta x_{l,0} + \Delta x_{l,l-r+1} = x_{l,l-r} \\ l^\alpha \Delta x_{l,0} + (r-1)^\alpha \Delta x_{l,l-r+1} = r^\alpha x_{l,l-r} \end{cases} \Rightarrow \begin{cases} \Delta x_{l,l-r+1} = \frac{l^\alpha - r^\alpha}{l^\alpha - (r-1)^\alpha} x_{l,l-r} \\ \Delta x_{l,0} = \frac{r^\alpha - (r-1)^\alpha}{l^\alpha - (r-1)^\alpha} x_{l,l-r} \end{cases} \tag{2.24}$$

After this traffic rerouting, the power consumed by layer l does not change. However, the incoming traffic of layer $l - r + 1$ has been increased. Therefore we need to adjust layer $l-r+1$'s traffic too. We intend to keep the power consumption of layer $l-r+1$ the same, so we try to increase $x_{l-r+1,l-r}$ by $\Delta x_{l-r+1,l-r}$ and decrease

$x_{l-r+1,0}$ by $\Delta x_{l-r+1,0}$. Traffic conservation and power consumption invariance imply that

$$\begin{cases} \Delta x_{l-r+1,l-r} - \Delta x_{l-r+1,0} = \frac{2l-1}{2l-2r+1}\Delta x_{l,l-r+1} \\ \Delta x_{l-r+1,l-r} = (l-r+1)^{\alpha}\Delta x_{l-r+1,0} \end{cases}$$

$$\Rightarrow \begin{cases} \Delta x_{l-r+1,l-r} = \frac{(l-r+1)^{\alpha}}{(l-r+1)^{\alpha}-1} \cdot \frac{2l-1}{2l-2r+1} \cdot \Delta x_{l,l-r+1} \\ \Delta x_{l-r+1,0} = \frac{1}{(l-r+1)^{\alpha}-1} \cdot \frac{2l-1}{2l-2r+1} \cdot \Delta x_{l,n-r+1} \end{cases} \tag{2.25}$$

Then there are two possible scenarios:

- Scenario I: $\Delta x_{l-r+1,0} \leq x_{l-r+1,0}$
- Scenario II: $\Delta x_{l-r+1,0} > x_{l-r+1,0}$

For scenario I, $\{x_{i,j}\}$ is updated as follows:

$$\begin{aligned} x^1_{l,l-r} &= 0 \\ x^1_{l,l-r+1} &= x_{l,l-r+1} + \Delta x_{l,l-r+1} \\ x^1_{l,0} &= x_{l,0} + \Delta x_{l,0} \\ x^1_{l-r+1,l-r} &= x_{l-r+1,l-r} + \Delta x_{l-r+1,l-r} \\ x^1_{l-r+1,0} &= x_{l-r+1,0} - \Delta x_{l-r+1,0} \\ x^1_{i,j} &= x_{i,j}, \text{for other } i,j \text{ and } i > l-r \\ x^1_{i,j} &= \frac{\sum_{k=i+1}^{L} \frac{2k-1}{2i-1} x^1_{k,i} + g}{\sum_{k=i+1}^{L} \frac{2k-1}{2i-1} x_{k,i} + g} x_{i,j}, i \leq l-r \end{aligned}$$

After updating, the traffic for layers beyond $l-r+1$ stays the same except layer l, so their power consumption do not change. The power consumption of layers l and $l-r+1$ does not change, and the incoming traffic of layer $l-r$ is changed by $\frac{2l-2r+1}{2l-2r-1}\Delta x_{l-r+1,l-r} - \frac{2l-1}{2l-2r-1}x_{l,l-r} = \frac{2l-1}{2l-2r-1}(\frac{(l-r+1)^{\alpha}}{(l-r+1)^{\alpha}-1} \cdot \frac{l^{\alpha}-r^{\alpha}}{l^{\alpha}-(r-1)^{\alpha}} - 1)x_{l,l-r}$. If $\frac{(l-r+1)^{\alpha}}{(l-r+1)^{\alpha}-1} \cdot \frac{l^{\alpha}-r^{\alpha}}{l^{\alpha}-(r-1)^{\alpha}} \leq 1$, the incoming traffic of layer $l-r$ will not increase.

Thus, the power consumption of layer $l-r$ will not increase. Now, we show $\frac{(l-r+1)^\alpha}{(l-r+1)^\alpha-1} \cdot \frac{l^\alpha-r^\alpha}{l^\alpha-(r-1)^\alpha} \leq 1$.

$$\begin{aligned} & \frac{(l-r+1)^\alpha}{(l-r+1)^\alpha-1} \cdot \frac{l^\alpha-r^\alpha}{l^\alpha-(r-1)^\alpha} \leq 1 \\ \Leftrightarrow \quad & [(l-r+1)r]^\alpha + (r-1)^\alpha \geq [(l-r+1)(r-1)]^\alpha + l^\alpha \end{aligned} \tag{2.26}$$

Noting that $(l-r+1)r+r-1 = (l-r+1)(r-1)+l = C$ where C is constant, equation (2.26) is equivalent to

$$(C-r+1)^\alpha + (r-1)^\alpha \geq (C-l)^\alpha + l^\alpha \tag{2.27}$$

Consider the function $f(x) = (C-x)^\alpha + x^\alpha$. This function is convex since $f''(x) \geq 0$ when $\alpha > 1$ and it is symmetric about $x = \frac{C}{2}$. It is easy to verify that the larger the value of $|C-2x|$, the larger the value of $f(x)$. Further $f(x)$ is strictly increasing with $|C-2x|$ when $\alpha > 1$. So the inequality (2.26) is equivalent to

$$|(l-r+1)r-(r-1)| \geq |(l-r+1)(r-1)-l| \tag{2.28}$$

It is easy to check that inequality (2.28) holds for all $2 < l \leq L, 1 < r < l$, so $\frac{(l-r+1)^\alpha}{(l-r+1)^\alpha-1} \cdot \frac{l^\alpha-l^\alpha}{l^\alpha-(r-1)^\alpha} \leq 1$, and $\frac{2l-ar+1}{2l-2r-1}\Delta x_{l-r+1,l-r} \leq \frac{2l-1}{2l-2r-1}x_{l,l-r}$, that is, the incoming traffic of layer $l-r$ does not increase. We then recursively update the traffic from layer $l-r$ to layer 1. Since the incoming traffic for layer $l-r$ does not increase, the traffic for all layers 1 to $l-r$ do not increase either, so their power consumption does not increase. Thus, the MIN-MAX power does not increase in scenario 1.

Actually, $|(l-r+1)r-(r-1)|$ is strictly greater than $|(l-r+1)(r-1)-l|$ when $2 < l \leq L, 1 < r < l$. So $\frac{(l-r+1)^\alpha}{(l-r+1)^\alpha-1} \cdot \frac{l^\alpha-l^\alpha}{l^\alpha-(r-1)^\alpha} < 1$, which means the incoming traffic and power consumption of layer $l-r$ are actually decreased.

Now let us consider scenario II: $\Delta x_{l-r+1,0} > x_{l-r+1,0}$. In this scenario, we cannot decrease $x_{l-r+1,0}$ by the whole amount $\Delta x_{l-r+1,0}$. Consequently, $\{x_{i,j}\}$ is updated as follows:

$$\begin{aligned}
x^1_{l,l-r} &= 0 \\
x^1_{l,l-r+1} &= x_{l,l-r+1} + \Delta x_{l,l-r+1} \\
x^1_{l,0} &= x_{l,0} + \Delta x_{l,0} \\
x^1_{l-r+1,l-r} &= x_{l-r+1,l-r} + x_{l-r+1,0} + \frac{2l-1}{2l-2r+1}\Delta x_{l,l-r+1} \\
x^1_{l-r+1,0} &= 0 \\
x^1_{i,j} &= x_{i,j}, \text{for other } i,j \text{ and } i > l-r \\
x^1_{i,j} &= \frac{\sum_{k=i+1}^{L} \frac{2k-1}{2i-1} x^1_{k,i} + g}{\sum_{k=i+1}^{L} \frac{2k-1}{2i-1} x_{k,i} + g} x_{i,j}, i \le l-r
\end{aligned}$$

After updating, the power consumption of layer l stays the same. The power consumption of layer $l-r+1$ is

$$P^1_{l-r+1} = x_{l-r+1,l-r} + x_{l-r+1,0} + \frac{2l-1}{2l-2r+1}\Delta x_{l,l-r+1}.$$

Next we will show $P^1_{l-r+1} \le P_{l-r}$. Since $\Delta x_{l-r+1,0} > x_{l-r+1,0}$, we have

$$\begin{aligned}
& x_{l-r+1,0} + \frac{2l-1}{2l-2r+1}\Delta x_{l,l-r+1} < \Delta x_{l-r+1,0} + \frac{2l-1}{2l-2r+1}\Delta x_{l,l-r+1} \\
= \;& \Delta x_{l-r+1,l-r} \le \frac{2l-1}{2l-2r+1} x_{l,l-r}, \qquad (2.29)
\end{aligned}$$

where the last equality is from Eqn. (2.25) and the last inequality comes from scenario I. We then have

$$P^1_{l-r+1} < x_{l-r+1,l-r} + \frac{2l-1}{2l-2r+1} x_{l,l-r} < P_{l-r} \qquad (2.30)$$

So the power consumption of layer $l-r+1$, P^1_{l-r+1}, is smaller than the original MIN-MAX power.

The incoming traffic of layer $l-r$ is changed by $x_{l-r+1,0} + \frac{2l-1}{2l-2r+1}\Delta x_{l,l-r+1} - \frac{2l-1.}{2l-2r-1}x_{l,l-r} < 0$. Thus, the incoming traffic of layer $l-r$ is decreased, so the power consumption of layer $l-r$ will not increase. The power consumption of all other layers do not increase either. Therefore, in scenario 2, after updating, the MIN-MAX power does not increase either.

Thus, after this procedure, $\{x_{i,j}\}$ is updated to $\{x^1_{i,j}\}$ by redistributing traffic on links to delete the traffic on $(l, l-r)$, and the MIN-MAX power does not increase. We keep executing this procedure until the solution is in the standard form. Since each application of this procedure does not increase the MIN-MAX power, the theorem is proved. □

Further, the standard form solution (2.22) is the unique solution for LP (2.8)-(2.13).

Lemma 2.3 *In any optimal solution for the optimization problem (2.8)-(2.13), the nodes in all layers will use energy at the same rate.*

Proof:

Suppose in an optimal solution, the nodes in different layers use the energy at different rate. Considering the innermost layer j from those layers with the highest energy consumption rate, there are two cases:

(i) If $j \geq 2$, let the energy consumption rate for nodes in layers j and $j-1$ be p_1 and p_2 respectively. Let the nodes in layer j send $0 < \Delta x < \frac{(p_1-p_2)(2j-3)}{(j-1)^\alpha(2j-1)}$ more traffic to layer $j-1$ and the nodes in layer $j-1$ send $\frac{2j-1}{2j-3}\Delta x$ more traffic to the sink. In this way the nodes in the layer j will reduce their energy consumption rate, and the nodes in the layer $j-1$ will increase their energy consumption rate but it remains smaller than p_1. Notice that since all nodes have the same initial energy and same traffic generation rate, this adjustment is always applicable. By

applying this adjustment iteratively, the MIN-MAX power will be reduced, thus the original optimal solution is not optimal, contradiction;

(ii) If $j = 1$, we denote layer i as the layer where all layers between layer 1 and layer i (including layer 1 and layer i) have the same energy consumption rate and layer $i+1$ has smaller energy consumption rate. Let the energy consumption rate for nodes in layers i and $i+1$ be p_1 and p_2 respectively. Let the nodes in layer $i+1$ send $0 < \Delta x < \frac{(p_1-p_2)}{(i+1)^\alpha - 1}$ more traffic to the sink, so the nodes in layer i have less relay traffic. In this way the nodes in the layer i will reduce their energy consumption rate, and the nodes in the layer $i+1$ will increase their energy consumption rate but the rate remains smaller than p_1. Similar to case (i) this leads to a contradiction. □

Corollary 2.4 *When $\alpha > 1$,the optimal standard form (2.22) solution is the unique optimal solution to the optimization problem (2.8)-(2.13)*

Proof:

According to the proof for Theorem 2.2, any solution can be transformed into standard form without decreasing the network lifetime. During the transformation, there always exist some layers whose energy consumption rate is lowered. It indicates that any other solution form except standard form cannot be optimal solution according to Lemma 2.3. And it is readily verified that there only exists one standard form optimal solution. □

Similar to two-dimensional case, we have following theorem for one-dimensional case.

Theorem 2.5 *When $\alpha > 1$, and each node can reach the sink by adjusting its transmission power, there always exists an optimal solution to the optimization*

problem (2.2)-(2.7) with the standard form (2.22).

Lemma 2.6 *In any optimal solution for the optimization problem (2.2)-(2.7), the nodes in all layers will use energy at the same rate.*

Corollary 2.7 *When $\alpha > 1$,the optimal standard form (2.22) solution is the unique optimal solution to the optimization problem (2.2)-(2.7)*

2.4 Summary

In this chapter, we have studied the lifetime maximization problem without considering processing and receiving energy consumption. We investigated both one dimensional network and two dimensional network. We modeled the problem into a linear program problem and studied the numerical results. The numerical results show that the proposed adaptive traffic distribution and transmission range adjustment scheme brings significant gain. The numerical results obtained also suggest a surprising conjecture, namely that if a node can reach the sink directly, the optimal way for it to split the traffic is to either send to the next layer toward the sink (i.e., using the minimum transmission range) or send directly to the sink. We then theoretically analyze this optimization problem and prove the conjecture.

Chapter 3

Wireless Sensor Network Lifetime Maximization With Receiving & Processing Power

In Chapter 2, we studied the lifetime maximizing problem without considering processing energy. When no processing energy consumption is considered, due to the nonlinear (e.g., quadratic for $\alpha = 2$) increase of transmission power consumption with respect to the transmission range, shorter transmission range is usually preferred. In other words, as long as the network connectivity can be maintained and certain QoS requirements can be satisfied, the smaller the value of r_{min}, the higher the energy efficiency per bit per meter, and consequently the higher the maximum achievable lifetime extension. However, when processing energy consumption is also considered, shorter transmission range may not always be preferred to longer transmission range.

In this chapter, we study the network lifetime maximization problem under a more general setting by incorporating the processing and receiving energy into

the model. The rest of this chapter is organized as follows. Section 3.1 describes the modified system model and re-formulated the network lifetime optimization under the new model. Section 3.2 presents the numerical results to the modified optimization problem, which is followed by the theoretical analysis. In Section 3.3 a fully distribution algorithm is proposed to let nodes adaptively distribute traffic and adjust transmission range. The simulation results are demonstrated in Section 3.4. Finally, Section 3.5 summarizes this chapter.

3.1 System Model and Problem Formulation

Same as the model in Chapter 2, we assume that all sensors have the same amount of initial energy, denoted by E. Each node has a minimum and maximum transmission range limitation denoted by r_{min} and r_{max}.

The transmission energy consumption at each node is modeled as follows:

$$P_t(r) = \beta \cdot r^{\alpha} \quad \text{per bit.} \tag{3.1}$$

Here α is the path loss exponent, r is the targeted transmission range, and β is a scalar indicating the energy needed to successfully convey an information bit to a unit distance.

Besides transmission energy consumption, circuit-level energy consumption, such as energy consumed during encoding, decoding, modulation, and demodulation, also plays an important role in many scenarios. In this work we refer to this as the processing energy. We first consider processing energy consumed during transmission. In general this contributes a constant additive term to the overall energy consumption, which can be modeled as follows:

$$P_c = \gamma_1 \quad \text{per bit.} \tag{3.2}$$

The value of γ_1 is determined by the underlying communication technologies, such as the encoding and modulation schemes used. Similarly, the processing energy consumed per bit during receiving stage is modeled as follows:

$$P_r = \gamma_2 \quad \text{per bit.} \tag{3.3}$$

The value of γ_2 is also determined by the underlying technologies, such as the decoding and demodulation schemes used.

Next we model the lifetime maximization problem with processing energy. To make the problem tractable, in this work we first focus on a sensor network deployed inside a circular area with the sink located in the center. Same as Chapter 2, we divide the network into multiple layers. Then we can model the lifetime maximization problem as follows:

$$\min_{\{x_{l,k},\ 1\le l\le L,\ 0\le k\le L\}} P \qquad s.t. \tag{3.4}$$

$$\sum_{k=l+1}^{L} \frac{2k-1}{2l-1} x_{k,l} + g = \sum_{k=0}^{l-1} x_{l,k}, \qquad 1 \le l \le L \tag{3.5}$$

$$\sum_{k=0}^{l-1} x_{l,k} P_t^{l,k} + \sum_{k=l+1}^{L} \frac{2k-1}{2l-1} x_{k,l} P_r \le P, \quad 1 \le l \le L \tag{3.6}$$

$$x_{l,k} \ge 0, \qquad 0 \le k < l, \quad 1 \le l \le L \tag{3.7}$$

$$x_{l,k} = 0, \qquad (l-k) r_{min} > r_{max}, 0 \le l, k \le L \tag{3.8}$$

$$x_{l,k} = 0, \qquad 0 \le l \le k \le L \tag{3.9}$$

where $P_t^{l,k} = P_c + P_t((l-k)r_{min})$. Eqn. (3.5) models the traffic conservation, i.e., for each node the amount of transmitted traffic should be equal to the traffic received plus the traffic generated. Eqn. (3.6) poses the energy constraint. Eqn. (3.7) guarantees the feasibility of the solutions. Eqn. (3.8) limits each node's maximum transmission range. Eqn. (3.9) prevents nodes from sending traffic further away from the sink.

3.2 Numerical Results and Theoretical Analysis

Now we study the effect of processing energy consumption on the lifetime maximization problem (3.4)-(3.9). When no processing energy consumption is considered, due to the nonlinear (e.g., quadratic for $\alpha = 2$) increase of transmission power consumption with respect to the transmission range, shorter transmission range is usually preferred. In other words, as long as the network connectivity can be maintained and certain QoS requirements can be satisfied, the smaller the value of r_{min}, the higher the energy efficiency per bit per meter, and consequently the higher the maximum achievable lifetime extension. However, when processing energy consumption is also considered, shorter transmission range may not always be preferred to longer transmission range. Instead, there exists an optimal transmission range such that the energy consumption per bit per meter is minimized, which is referred to as the characteristic distance [5]. In our model, it is easy to check that the characteristic distance d_{char} is:

$$d_{char} = \left(\frac{\gamma_1 + \gamma_2}{\beta(\alpha - 1)} \right)^{\frac{1}{\alpha}}. \tag{3.10}$$

Later we will see that d_{char} plays a critical role in the solution to the optimization problem (3.4)-(3.9).

In order to obtain the optimal solution to (3.4)-(3.9), our first step is to apply numerical analysis. To make the results solid, our analysis is based on the typical energy consumption parameters as well as their variations [5,24]. To have a better understanding of how processing energy consumption affects the results, we impose different constraints on the original problem (3.4)-(3.9). Specifically, four sets of constraints are imposed separately, as described in Table 3.1. To compare the lifetime obtained under different constraints, we regard the lifetime obtained by imposing constraint C1 as the baseline.

Table 3.1: Extra constraints imposed on the original problem (3.4)-(3.9)

C1:	always transmit using r_{min}.
C2:	always transmit using d_{char}.
C3:	either transmit using d_{char}, or directly to the sink.
C4:	no extra constraint.

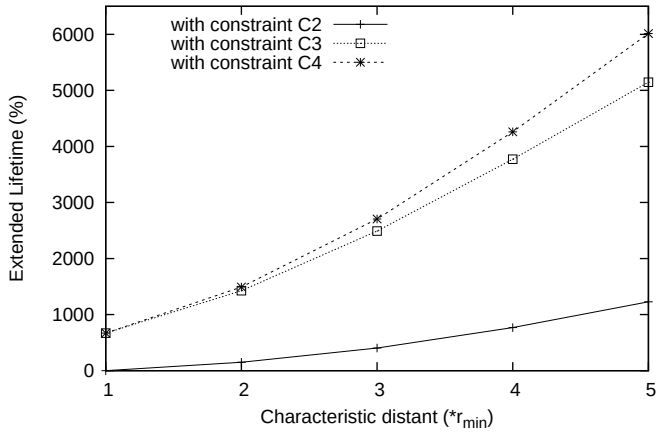

Figure 3.1: Lifetime comparison among different scenarios. Both r_{min} and the network radius are fixed. $\alpha = 2$

We set $\gamma_1 = 45\text{nJ/bit}$, $\gamma_2 = 135\text{nJ/bit}$, and $\beta = 10\text{pJ/bit}/m^2$ for $\alpha = 2$ [24]. Thus, $d_{char} \simeq 134m$. We then fix r_{min} to be the characteristic distances calculated based on the above parameters, and decrease the value of β to get different characteristic distances. Such decrease happens when the receiving technologies advances, or when some special decoding techniques are applied. We fix $R = 20r_{min}$. Fig. 3.1 illustrates the results obtained by imposing different constraints.

First, Fig. 3.1 shows that dramatic lifetime extension can be achieved by C3 and C4. For example, when $d_{char} = r_{min}$, more than 700% extension is achieved, while when $d_{char} = 5r_{min}$, the lifetime extension can be up to 5000%. The results indicate

that instead of decreasing the effectiveness of the adaptive traffic distribution and power control approach, the introduction of processing energy consumption can even further increase the maximum achievable network lifetime extension. Second, we can see that the lifetime extension also increases with the increase of characteristic distance. For example, even for C2, when $d_{char} = 5r_{min}$, the lifetime extension can reach 1200%. This suggests that transmitting using characteristic distance is much more energy efficient than transmitting using r_{min}. In other words, shorter transmission range is not always preferred when the processing energy consumption is taken into account. When processing energy consumption plays a more important role in overall energy consumption (i.e., $\frac{\gamma_1+\gamma_2}{\beta}$ increases), transmitting using a short range becomes less energy efficient per bit per meter.

After examining the numerical solutions, we observe that when no extra constraint is imposed (corresponding to C4), in most situations each node either directly transmits the traffic to the sink, or to some inner layers around d_{char} away. This also explains why the lifetime gap between C3 and C4 is small, where the lifetime obtained by imposing C4 is only slightly longer than the lifetime obtained by imposing C3. Due to its simplicity and the concern of distributed implementation, the constraint C3 is usually preferred.

So far when we have changed d_{char}, we fixed the values of γ_1 and γ_2. However, with the advance of technology, both γ_1 and γ_2 may change. For example, applying sophisticated decoding techniques may lead to the increase of γ_2, while applying sophisticated encoding techniques may increase γ_1, and either can lead to the decrease of β. Now the question is whether the change of γ_1 and γ_2 will result in the dramatic change of the solutions. To study this issue, we consider the following three scenarios when increasing d_{char}: 1) simultaneously increase γ_1 and

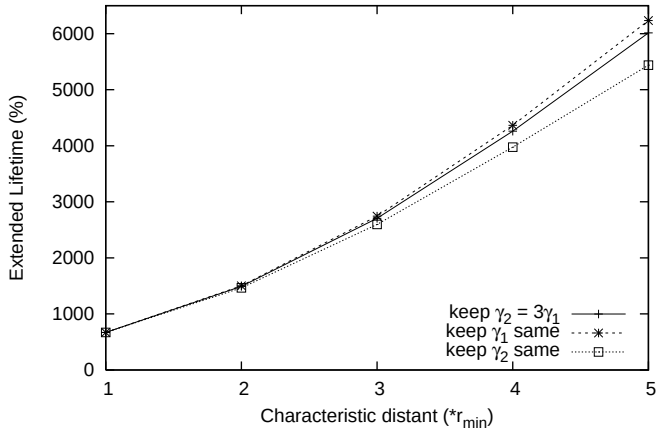

Figure 3.2: Lifetime extension comparison by varying the ratio of γ_1/γ_2, $\alpha = 2$.

γ_2 by keeping $\gamma_1/\gamma_2 = 1/3$; 2) increase γ_2 only by fixing γ_1; 3) increase γ_1 only by fixing γ_2. Fig. 3.2 illustrates the numerical results obtained under 3 different scenarios by applying constraint C4. From Fig. 3.2 we can see that although the maximum achievable lifetime extension is slightly different among the three scenarios, the three curves look very similar. This suggests that varying γ_1 and γ_2 will not affect the effectiveness of the adaptive traffic distribution and power control approach.

In the above analysis we focus on studying the effect of different transmitting and receiving technologies (i.e., different γ_1, γ_2 and β settings). Now we fix the values of γ_1, γ_2, and β, and study the effect of r_{min}. As we mentioned before, besides physical limitation, r_{min} is also determined by certain QoS requirements, such as network connectivity. For example, in a dense network we can use a small r_{min}, while in a sparse network we need a large r_{min} to maintain necessary connectivity. Fig. 3.3 illustrates the results for various r_{min}. As before, we set $\alpha = 2$, $\gamma_1 = 45$nJ/bit, $\gamma_2 = 135$nJ/bit, $\beta = 10$pJ/bit/m^2. Two network sizes are

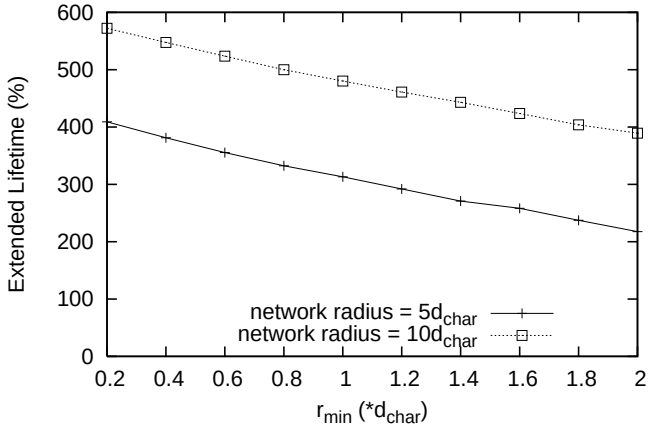

Figure 3.3: Lifetime comparison for different network size $5 * d_{char}$ and $10 * d_{char}$ by fixing d_{char} and changing r_{min}, $\alpha = 2$.

studied: $10d_{char}$ and $5d_{char}$. Since we have observed that imposing constraint C1 is not energy efficient, here we use the lifetime obtained by imposing constraint C2 as baseline. The results illustrated in Fig. 3.3 show the extended lifetime obtained by imposing no extra constraints (C4).

First, Fig. 3.3 shows that higher lifetime extension can be obtained with the increase of network size. This is similar to the results illustrated in Fig. 2.2. Second, with the decrease of r_{min}, the extensible lifetime increases. This is because smaller r_{min} allows nodes to adjust their transmission power in a finer way since r_{min} is the width of each layer. On the other hand, though the extensible lifetime decreases when r_{min} increases, there is still considerable lifetime extension available. For example, when the network size is $10d_{char}$ and r_{min} is $2d_{char}$, the extended lifetime is about 400%. This also suggests that the approach of adaptive traffic distribution and power control effectively extend the network lifetime under different network size and node density.

When we further examine the numerical solutions to optimization problem (3.4)-(3.9), we find that when $r_{min} \geq 1.2d_{char}$, the optimal solution also exhibits a standard form. This has been generalized by the following theorem:

Theorem 3.1 *When all nodes can reach the sink by adjusting their transmission power, as long as* $\frac{r_{min}}{d_{char}} \geq \max\{(\frac{(\alpha-1)(l^\alpha - r^\alpha)}{[r(l-r+1)]^\alpha + (r-1)^\alpha - l^\alpha - [(l-r+1)\cdot(r-1)]^\alpha})^{\frac{1}{\alpha}},\ 3 \leq l \leq L,\ 2 \leq r \leq l-1\}$*, there always exists an optimal solution to the problem (3.4)-(3.9) with the standard form (2.22).*

Proof:

We let $r_{min} = c \cdot d_{char}$, where c is constant. Then $P_t^{l,k} = \gamma_1 + \beta((l-k)cd_{char})^\alpha = \gamma_1 + \frac{\gamma_1+\gamma_2}{\alpha-1} \cdot (c(l-k))^\alpha$. We will show that any optimal solution can be transformed into a solution in standard form without losing optimality.

Let $\{x_{i,j}\}$ be an optimal solution. If this optimal solution is not in the standard form, then we can transform $\{x_{i,j}\}$ to $\{\tilde{x}_{i,j}\}$ such that $\{\tilde{x}_{i,j}\}$ is in the standard form (2.22). The whole procedure is as follows:

We iteratively apply the following procedure: find the first link $x_{l,l-r}$ with the following properties:

- $\{x_{i,i-1} \geq 0, x_{i,0} \geq 0, x_{i,j} = 0, 0 < i < l, 1 \leq j \leq i-2\}$, that is, for all $i < l$, except $x_{i,0}$ and $x_{i,i-1}$, no other links can have non-zero value.
- For all $0 < j < l - r$, $x_{l,j} = 0$.

Next we show how to redistribute $x_{l,l-r}$ to the other links without increasing the MIN-MAX power. For layer $l - r$, its initial power is:

$$\begin{aligned} P_{l-r} &= x_{l-r,0}P_t^{l-r,0} + x_{l-r,l-r-1}P_t^{l-r,l-r-1} + P_r \sum_{i=l-r+1}^{L} \frac{2i-1}{2l-2r-1} x_{i,l-r} \\ &\geq (P_t^{l-r,l-r-1} + P_r)\left(\frac{x_{l-r+1,l-r}(2l-2r+1)}{2l-2r-1} + \frac{x_{l,l-r}(2l-1)}{2l-2r-1} + \sum_{i=l+1}^{L} \frac{2i-1}{2l-2r-1} x_{i,l-r}\right) \end{aligned} \tag{3.11}$$

where $\frac{x_{l-r+1,l-r}(2l-2r+1)}{2l-2r-1} + \frac{x_{l,l-r}(2l-1)}{2l-2r-1} + \sum_{i=l+1}^{L} \frac{2i-1}{2l-2r-1} x_{i,l-r} + g = x_{l-r,0} + x_{l-r,l-r-1}$ is the traffic that layer $l-r$ needs to transmit.

We split traffic $x_{l,l-r}$ into two parts $\Delta x_{l,l-r+1}$ and $\Delta x_{l,0}$ which will be sent to the layer $l-r+1$ and the sink respectively. To conserve traffic and to keep the layer l power consumption unchanged, we need to have

$$\begin{cases} \Delta x_{l,0} + \Delta x_{l,l-r+1} = x_{l,l-r} \\ P_t^{l,0} \Delta x_{l,0} + P_t^{l,l-r+1} \Delta x_{l,l-r+1} = P_t^{l,l-r} x_{l,l-r} \end{cases}$$

$$\Rightarrow \begin{cases} \Delta x_{l,l-r+1} = \frac{l^\alpha - r^\alpha}{l^\alpha - (r-1)^\alpha} x_{l,l-r} \\ \Delta x_{l,0} = \frac{r^\alpha - (r-1)^\alpha}{l^\alpha - (r-1)^\alpha} x_{l,l-r} \end{cases} \tag{3.12}$$

After this traffic rerouting, the power consumed by layer l does not change. However, the incoming traffic of layer $l-r+1$ has been increased. Therefore we need to adjust layer $l-r+1$'s traffic too. We intend to keep the power consumption of layer $l-r+1$ the same, so we try to increase $x_{l-r+1,l-r}$ by $\Delta x_{l-r+1,l-r}$ and decrease $x_{l-r+1,0}$ by $\Delta x_{l-r+1,0}$. Traffic conservation and power consumption invariance imply that

$$\begin{cases} \Delta x_{l-r+1,l-r} - \Delta x_{l-r+1,0} = \frac{2l-1}{2l-2r+1} \Delta x_{l,l-r+1} \\ P_t^{l-r+1,l-r} \Delta x_{l-r+1,l-r} + P_r \frac{2l-1}{2l-2r+1} \Delta x_{l,l-r+1} = P_t^{l-r+1,0} \Delta x_{l-r+1,0} \end{cases}$$

$$\Rightarrow \begin{cases} \Delta x_{l-r+1,l-r} = \frac{\alpha - 1 + (c(l-r+1))^\alpha}{(c(l-r+1))^\alpha - c^\alpha} \frac{2l-1}{2l-2r+1} \Delta x_{l,l-r+1} \\ \Delta x_{l-r+1,0} = \frac{\alpha - 1 + c^\alpha}{(c(l-r+1))^\alpha - c^\alpha} \frac{2l-1}{2l-2r+1} \Delta x_{l,l-r+1} \end{cases} \tag{3.13}$$

Then there are two possible scenarios:

- Scenario 1: $\Delta x_{l-r+1,0} \leq x_{l-r+1,0}$
- Scenario 2: $\Delta x_{l-r+1,0} > x_{l-r+1,0}$

For scenario 1, $\{x_{i,j}\}$ is updated as follows:

$$\begin{aligned}
x^1_{l,l-r} &= 0 \\
x^1_{l,l-r+1} &= x_{l,l-r+1} + \Delta x_{l,l-r+1} \\
x^1_{l,0} &= x_{l,0} + \Delta x_{l,0} \\
x^1_{l-r+1,l-r} &= x_{l-r+1,l-r} + \Delta x_{l-r+1,l-r} \\
x^1_{l-r+1,0} &= x_{l-r+1,0} - \Delta x_{l-r+1,0} \\
x^1_{i,j} &= x_{i,j}, \text{for other } i,j \text{ and } i > l-r \\
x^1_{i,j} &= \frac{\sum_{k=i+1}^{L} \frac{2k-1}{2i-1} x^1_{k,i} + g}{\sum_{k=i+1}^{L} \frac{2k-1}{2i-1} x_{k,i} + g} x_{i,j}, i \le l-r
\end{aligned}$$

After updating, the traffic for layers beyond $l-r+1$ stays the same except layer l, so their power consumptions do not change. The power consumptions of layers l and $l-r+1$ do not change, and the incoming traffic of layer $l-r$ is changed by $\frac{2l-2r+1}{2l-2r-1}\Delta x_{l-r+1,l-r} - \frac{2l-1}{2l-2r-1}x_{l,l-r} = \frac{2l-1}{2l-2r-1}(\frac{\alpha-1+(c(l-r+1))^\alpha}{(c(l-r+1))^\alpha - c^\alpha} \cdot \frac{l^\alpha - r^\alpha}{l^\alpha-(r-1)^\alpha} - 1)x_{l,l-r}$. If $\frac{\alpha-1+(c(l-r+1))^\alpha}{(c(l-r+1))^\alpha - c^\alpha} \cdot \frac{l^\alpha - r^\alpha}{l^\alpha-(r-1)^\alpha} \le 1$, the incoming traffic of layer $l-r$ will not increase. It is readily verified that

$$\frac{\alpha-1+(c(l-r+1))^\alpha}{(c(l-r+1))^\alpha - c^\alpha} \cdot \frac{l^\alpha - r^\alpha}{l^\alpha-(r-1)^\alpha} \le 1 \Leftrightarrow$$

$$c \ge \left(\frac{(\alpha-1)(l^\alpha - r^\alpha)}{[r(l-r+1)]^\alpha + (r-1)^\alpha - l^\alpha - [(l-r+1)\cdot(r-1)]^\alpha} \right)^{\frac{1}{\alpha}}$$

Thus the incoming traffic of layer $l-r$ and the layers inside layer $l-r$ will not increase, so the MIN-MAX power will not increase.

Now let us consider scenario 2: $\Delta x_{l-r+1,0} > x_{l-r+1,0}$. In this scenario, we cannot decrease $x_{l-r+1,0}$ by the whole amount $\Delta x_{l-r+1,0}$. Consequently, $\{x_{i,j}\}$ is updated

as follows:

$$\begin{aligned}
x^1_{l,l-r} &= 0 \\
x^1_{l,l-r+1} &= x_{l,l-r+1} + \Delta x_{l,l-r+1} \\
x^1_{l,0} &= x_{l,0} + \Delta x_{l,0} \\
x^1_{l-r+1,l-r} &= x_{l-r+1,l-r} + x_{l-r+1,0} + \frac{2l-1}{2l-2r+1}\Delta x_{l,l-r+1} \\
x^1_{l-r+1,0} &= 0 \\
x^1_{i,j} &= x_{i,j}, \text{ for other } i,j \text{ and } i > l-r \\
x^1_{i,j} &= \frac{\sum_{k=i+1}^{L} \frac{2k-1}{2i-1} x^1_{k,i} + g}{\sum_{k=i+1}^{L} \frac{2k-1}{2i-1} x_{k,i} + g} x_{i,j}, \ i \le l-r
\end{aligned}$$

After updating, the power consumption of layer l stays the same. The power consumption of layer $l-r+1$ is

$$\begin{aligned}
P^1_{l-r+1} &= P_t^{l-r+1,l-r}(x_{l-r+1,l-r} + x_{l-r+1,0} + \frac{2l-1}{2l-2r+1}\Delta x_{l,l-r+1}) \\
&\quad + P_r(\sum_{k=l-r+1}^{L} \frac{2k-1}{2l-2r+1} x_{k,l-r+1} + \frac{2l-1}{2l-2r+1}\Delta x_{l,l-r+1}) \\
&\le (P_t^{l-r+1,l-r} + P_r)(x_{l-r+1,l-r} + x_{l-r+1,0} + \frac{2l-1}{2l-2r+1}\Delta x_{l,l-r+1})
\end{aligned}$$

Next we will show $P^1_{l-r+1} \le P_{l-r}$. Since $\Delta x_{l-r+1,0} > x_{l-r+1,0}$, we have

$$\begin{aligned}
& x_{l-r+1,0} + \frac{2l-1}{2l-2r+1}\Delta x_{l,l-r+1} < \Delta x_{l-r+1,0} + \frac{2l-1}{2l-2r+1}\Delta x_{l,l-r+1} \\
= \ & \Delta x_{l-r+1,l-r} \le \frac{2l-1}{2l-2r+1} x_{l,l-r}, \qquad (3.14)
\end{aligned}$$

where the final inequality has been obtained in scenario 1. We then have

$$P^1_{l-r+1} < (P_t^{l-r+1,l-r} + P_r)(x_{l-r+1,l-r} + \frac{2l-1}{2l-2r+1} x_{l,l-r}) \le P_{l-r} \qquad (3.15)$$

So the power consumption of layer $l-r+1$, P^1_{l-r+1}, is smaller than the original MIN-MAX power.

The incoming traffic of layer $l-r$ is changed by $\frac{2l-2r+1}{2l-2r-1}x_{l-r+1,0}+\frac{2l-1}{2l-2r-1}\Delta x_{l,l-r+1}-\frac{2l-1}{2l-2r-1}x_{l,l-r} < 0$. Thus, the incoming traffic of layer $l-r$ is decreased, so the power consumption of layer $l-r$ will not increase. The power consumptions of all other layers do not increase either. Therefore, in scenario 2, after updating, the MIN-MAX power does not increase either.

Thus, after this procedure, $\{x_{i,j}\}$ is updated to $\{x^1_{i,j}\}$ by redistributing traffic to delete the traffic on $(l, l-r)$, and the MIN-MAX power does not increase. We keep executing this procedure until the solution is in the standard form. Since each application of this procedure does not increase the MIN-MAX power, the theorem is proved. □

Theorem 3.1 shows that as long as the layer width is large enough –i.e., r_{min} is sufficient large– there is always an optimal solution in standard form. At the same time, according to Fig. 3.1, although the standard form solution is not optimal when r_{min} is small (relative to d_{char}), it can still approximate the optimal solution very well.

Corollary 3.2 *When all nodes can reach the sink by adjusting their transmission power, and $\alpha = 2$, as long as $\frac{r_{min}}{d_{char}} \geq \frac{\sqrt{5}}{2}$, there always exists an optimal solution to the problem (3.4)-(3.9) with the standard form (2.22).*

Proof:

When $\alpha = 2$,

$$\left(\frac{(\alpha-1)(l^\alpha - r^\alpha)}{[r(l-r+1)]^\alpha + (r-1)^\alpha - l^\alpha - [(l-r+1)\cdot(r-1)]^\alpha}\right)^{\frac{1}{\alpha}} = \left(\frac{l+r}{2(l-r+1)(r-1)}\right)^{\frac{1}{\alpha}}$$

Regarding r as constant, let $f(l) = \frac{l+r}{2(l-r+1)(r-1)}$, then we have

$$f(l) \geq f(l+1) \Leftrightarrow \frac{l+r}{2(l+1-r)(r-1)} \geq \frac{l+1+r}{2(l+1+1-r)(r-1)} \Leftrightarrow 2r \geq 1 \quad (3.16)$$

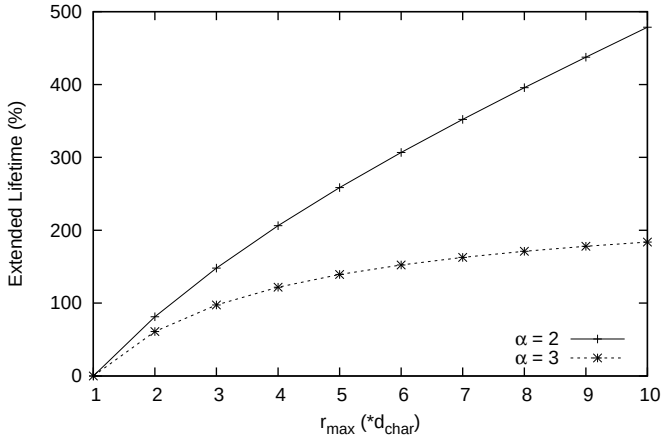

Figure 3.4: Lifetime extension for different r_{max} under extra constraint C5

So when r is fixed, $f(l)$ is a nonincreasing function.

Regarding l as constant, let $g(r) = \frac{l+r}{2(l-r+1)(r-1)}$, and let $l-3 \geq w \geq 1$, then we have

$$\begin{aligned} g(2) \geq g(2+w) &\Leftrightarrow \frac{l+2}{2(l-1)} \geq \frac{l+2+w}{2(l-w-1)(w+1)} \\ &\Leftrightarrow l^2 \geq lw + l + 2w + 3 \\ &\Leftrightarrow w \leq \frac{l^2-l-3}{l+2} \end{aligned} \tag{3.17}$$

At the same time, $l-3 \leq \frac{l^2-l-3}{l+2} \Leftrightarrow -3 \leq 0$. It guarantees that (3.17) holds when $w \leq l-3$. So the max of $g(r)$ is achieved at $r=2$.

Thus when $\alpha = 2, \max\{(\frac{(\alpha-1)(l^\alpha - r^\alpha)}{[r(l-r+1)]^\alpha + (r-1)^\alpha - l^\alpha - [(l-r+1)\cdot(r-1)]^\alpha})^{\frac{1}{\alpha}}, 3 \leq l \leq L, 2 \leq r \leq l-1\}$ is achieved at $l=3, r=2$ which makes it $\frac{\sqrt{5}}{2}$. According to Theorem 2, the corollary holds. □

As we mentioned before, allowing nodes to adaptively adjust transmission power and transmit using a long range may cause significant signal interference. In Chapter 2 we combat this issue by only allowing a small number of sensors that are nearest to the sink to adjust their transmission range, while all other nodes fix

their transmission range to be r_{min}. In this chapter we also adopt a similar approach with the difference being that now outside nodes will fix their transmission range to be d_{char}. Fig. 3.4 illustrates the results by limiting the number of nodes that are allowed to adjust transmission range. The baseline is the lifetime obtained by imposing constraint C2. The results are obtained by fixing the network size to be $10d_{char}$, setting $r_{min} = d_{char}$, changing r_{max}, using constraint C3, and imposing the extra constraint, denoted as C5, that only nodes which can directly reach the sink are allowed to adjust transmission range.

From the results presented in Fig. 3.4 we can see that even when only several innermost layers are allowed to adjust their transmission power, the lifetime extension can still be significant. When α is large, the performance loss compared to the case without the extra constraint is small. For example, when $\alpha = 3$, which is a typical path loss exponent value, by only allowing the innermost 3 layers to adjust transmission power, we can have 100% lifetime extension. The conclusion is similar to those obtained from Fig. 2.4 and Fig. 2.5. The difference is that the network lifetime extension has been increased by incorporating the processing energy consumption. As discussed before, the significance of the constraint C5 lies in that it can greatly simplify the distributed algorithm implementation and reduce the extra signal interference.

3.3 Distributed Algorithm

In Section 3.2 we found that imposing constraint C3 (either transmitting using d_{char} or to the sink directly) can significantly simplify the implementation without much performance loss. Further, in order to combat the negative effect of long transmission range, we impose the extra constraint C5: only those nodes that can

directly reach the sink are allowed to adjust their transmission range. As long as r_{max} is small, the extra signal interference caused by adaptive power adjustment will be limited. However, all these numerical results are obtained through centralized computation which is not appropriate for wireless sensor networks. For example, the randomness of the sensor locations may lead to big relay burden difference between nodes in the same layer, so it is not appropriate to assign a fixed splitting ratio to the sensors in the same layer.

In this section we propose *Energy Aware Data Propagation Algorithm* (EADPA), a fully distributed algorithm, to adaptively split traffic and adjust transmission power for each node. For a given node, if it is allowed to adjust its transmission range, it needs to determine how to split the traffic to be sent between the sink and the next relay respectively. It is not efficient to let some sensors relay a lot since it will make the network die fast. Thus when a node has higher residual energy than its relays, it should send the traffic directly to the sink.

The basic idea of EADPA is as follows: suppose each node has selected a set of nodes (possibly one) as its relays, where the relays are around d_{char} away from it. Each node keeps record of the residual energy of its relays. When a node has a packet to send, it first compares its residual energy to the residual energy of its relays. If its residual energy is more than the residual energy of all relays and it can directly reach the sink, then it sends the packet directly to the sink; otherwise, it sends the packet to one of the relays that has the maximum residual energy.

The algorithmic description of EADPA is illustrated in Algorithm 1. In Algorithm 1 we assume that for each node the set of its relays $\mathcal{P}$ has been given. This can be obtained in the following way: for each node, if the sink is within d_{char} distance, then set the sink as its only relay; otherwise, pick k nodes within its $c \cdot d_{char}$

distance, who have the shortest distances to the sink, as its relays. Here $k \geq 1$ and $c \geq 1$ are system parameters that can be determined empirically. Another issue is how a node monitors the residual energy of its relays. This can be done by letting all nodes broadcast their residual energy periodically.

Algorithm 1 Energy Aware Data Propagation Algorithm

Input: E denotes a node's initial energy, $\mathcal{P}$ denotes the set of its relays, r denotes its distance to the sink;

1: $E_{residual} = E$; $d = \min\{r, d_{char}\}$;
2: **while** $(E_{residual} > 0)$ **do**
3: Let T denote the total traffic needed to be sent this time;
4: **if** $(T \cdot (P_c + P_t(d)) > E_{residual})$ **then**
5: **break;**
6: **end if**
7: Find the relay p with the maximum residual energy from $\mathcal{P}$, and use $E^p_{residual}$ to denote p's residual energy;
8: **if** $(E^p_{residual} < E_{residual}$ AND $r \leq r_{max})$ **then**
9: Directly send the packet to the sink;
10: $E_{residual} = E_{residual} - T \cdot (P_c + P_t(r))$;
11: **else**
12: send the packet to p;
13: $E_{residual} = E_{residual} - T \cdot (P_c + P_t(d_{char}))$;
14: $E^p_{residual} = E^p_{residual} - T \cdot P_r$;
15: **if** $(E^p_{residual} < 0)$ **then**
16: **break;**
17: **end if**
18: **end if**
19: **end while**

Algorithm 1 describes the procedure for the data transaction. Most steps are executed by the sender except steps 14-17 which are executed by the receiver.

3.4 Simulation Results

This section evaluates the performance of proposed distributed algorithm EADPA, which is the distributed implementation of proposed adaptive traffic distribution and power control approach, in randomly deployed wireless sensor networks. In all simulations, for each sensor, we set $\gamma_1 = 45$nJ/bit, $\gamma_2 = 135$nJ/bit, $\beta = 10$pJ/bit/m^2 for $\alpha = 2$, therefore $d_{char} \simeq 134m$. We set $r_{min} = d_{char}$, and set the node density to be $25/\pi r_{min}^2$. Initially, each sensor has 2000 Joule energy. In each unit time (round) each node will generate a 25-Byte message to be sent to the sink. The network radius varies from 600m to 1000m. Next we evaluate the performance of the proposed EADPA algorithm. The baseline network lifetime is obtained by letting all sensors transmit using d_{char}. In the simulations, only the nodes that can reach the sink directly execute EADPA. We then set r_{max} to different values to test different scenarios.

We first focus on randomly deployed circular sensor network with radius R. The sink is located at the center of the area. Fig. 3.5 illustrates the simulation results, where the four curves correspond to the lifetime extension obtained under four different r_{max} settings: 300m, 400m, 500m, and R. It is worth pointing out that in our simulations, interference has not been considered separately.

First, from Fig. 3.5 we can see that after applying adaptive traffic distribution and power control, the network lifetime can be significantly extended. For example, when $r_{max} = R = 1000m$, more than 400% lifetime extension has been achieved, which also agrees with our numerical results. These results also confirm that even if only a small portion of nodes are allowed to adjust transmission range, the lifetime extension can still be significant. For example, when R = 1000m and $r_{max} = 300$m, only 9% of the nodes are allowed to adjust their transmission power, while 80%

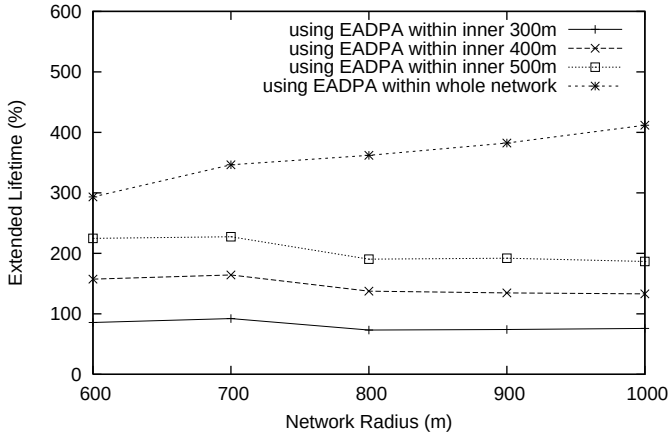

Figure 3.5: Lifetime extension for EADPA in circular network

lifetime extension can be achieved. Third, we can see that the lifetime extension is mainly determined by r_{max}, and changes little with the variation of network radius R, which also agrees with our numerical analysis.

Next we change the network area from circular to square. In this set of simulations, nodes are randomly deployed in a square with the sink lying in the center. The length of each edge is $2R$. The simulation results are illustrated in Fig. 3.6. Comparing the results in Fig. 3.6 with the results in Fig. 3.5, we can see that the results are almost identical except for some minor differences. One difference is that when $r_{max} = R$, the squared case results are slightly higher in lifetime extension due to the fact that more nodes are in the squared network. Another difference is that when $r_{max} < R$, the squared case results are slightly lower in lifetime extension since a smaller portion of nodes are allowed to adjust their transmission range in the squared case.

Finally let us consider the rectangular network. In this set of simulations, nodes are randomly deployed in a rectangle with the sink lying in the center. The size of

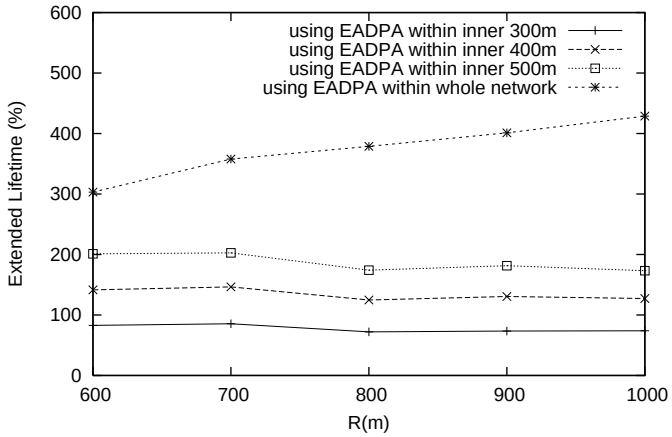

Figure 3.6: Lifetime extension for EADPA in squared network

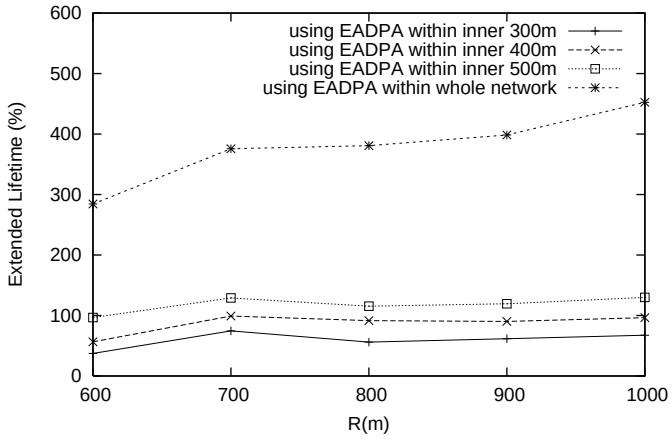

Figure 3.7: Lifetime extension for EADPA in rectangle network

the rectangle is $2R \times 4R$. The simulation results are illustrated in Fig. 3.7. From this figure, we can see that the maximum achievable lifetime extension is similar to the previous case. This confirms that the proposed scheme works well in rectangle too. We also observe that when $r_{max} < R$, the extension for the rectangle case is lower than the circular and squared cases. This is because when we only consider the several inner layers, the achievable lifetime extension mainly depends on the ratio between the number of the nodes allowed to adjust transmission range and the number of total nodes.

The above results show that the proposed distributed algorithm EADPA can work well in different shaped sensor networks.

3.5 Related work and Summary

In [20, 34, 49, 63], similar approaches have been studied to extend the network lifetime. There are several major differences between our work with these work. First, instead of maximizing the network lifetime, their goal is to let nodes die at the same time, which may lead to a suboptimal solution. Second, their work has not considered processing energy consumption, which limits their applicability. Third, they have only considered the situation that the path loss exponent is 2. Fourth, they do not provide any distributed algorithms, and all their solutions need to be calculated in a centralized way.

In this chapter we have demonstrated that adaptive traffic distribution and power control can significantly extend the lifetime of wireless sensor networks. We have also demonstrated that by incorporating the processing energy consumption, the lifetime can be further extended comparing to only considering the transmission energy consumption. When investigating the optimal solutions to the lifetime

maximizing adaptive traffic distribution and power control problem, one important finding is that nodes should either transmit in the most energy efficient way, or directly transmit to the sink. This has been verified by both numerical results as well as theoretical analysis. We have also shown that the network lifetime can still be dramatically extended even if only a small portion of innermost nodes are allowed to adjust their transmission power. This has great practical implication since it can significantly simplify the medium access control and scheduling protocol design. Finally, we have proposed a fully distributed algorithm to perform adaptive traffic distribution and transmission power adjustment for randomly deployed wireless sensor networks. Extensive simulation have also been conducted, and the results have demonstrated that the network lifetime can be dramatically extended by applying the proposed approach in various scenarios.

Chapter 4

Prolonging Network Lifetime via Partially Controlled Node Deployment and Adaptive Data Propagation

In Chapter 2 and Chapter 3, we have studied the lifetime maximizing problem for a fully deployed sensor network. In this chapter we will investigate how to maximize the network lifetime via joint optimization of node deployment and adaptive traffic distribution and power control. The rest of the chapter is organized as follows. Section 4.1 describes the network model and problem formulation. Section 4.2 presents the numerical results for the joint optimization problem. Section 4.3 provides the simulation studies. Finally Section 4.4 summarizes this chapter.

4.1 Network Model and Problem Formulation

In this chapter we consider the following flat circular wireless sensor network model. There are two types of wireless nodes in the network: sensors and relays. Each sensor needs to submit the collected information to the sink which is located in the center of the network. Relay nodes will not generate traffic, that is, relay nodes will only forward packets, but will not generate traffic. The sensor nodes are randomly deployed according to the uniform distribution with fixed density such that the network coverage constraint can be satisfied with high probability [41, 69]. Let N denote the total number of sensor nodes, which can be easily calculated. We consider the problem of deploying M relay nodes into the network in a partially controlled way to prolong the network lifetime. Here partially controlled way means that the relays cannot be deployed to specific positions controllably, but can be deployed with specific distribution density. Our objective is to find the optimal relay distribution achieving maximum network lifetime when sensor nodes have a fixed and nonrenewable battery.

We assume that all nodes (sensors and relays) have the same amount of initial energy, denoted by E. There is no energy constraint on the sink. Given the network to be deployed, some Quality of Service (QoS) requirements, and specific types of sensors, we also pose a minimum transmission range limitation for each sensor, denoted by r_{min}. The value of r_{min} can be determined by both hardware limitation and QoS requirements, such as network connectivity. We assume all nodes can adjust their transmission range as needed.

Same as before, we model the energy consumption at each node as follows:

$$P_t(r) = \gamma_1 + \beta \cdot r^{\alpha} \text{ per bit} \tag{4.1}$$

$$P_r = \gamma_2 \text{ per bit} \tag{4.2}$$

Here $P_t(r)$ is the processing and transmission energy consumption and P_r is the receiving energy consumption. γ_1 and γ_2 are constant which are determined by the underlying technology. α is the path loss exponent, which is determined by the environment. r is the targeted transmission range, and β is a scalar indicating the energy needed to successfully convey an information bit to a unit distance.

We assume that all nodes (sensors, relays and the sink) use a common frequency channel. Since the relay nodes do not produce traffic nor sense the environment, here we refer to network lifetime as the time elapsing between network deployment and the moment when the first sensor node dies.

To make the problem tractable, we follow the network model used in previous chapters. Specifically, the network is divided into multiple layers: a node belongs to the l^{th} layer if and only if its distance to the sink lies in the range $((l-1) \cdot r_{min}, l \cdot r_{min}]$, and the layer 0 is the sink. So the width for each layer is r_{min}.

Due to the symmetry of network topology and traffic pattern relative to the sink, intuitively relay nodes should be deployed in a symmetric way. When the network size is large and the number of relay nodes is not too small, deploying nodes in a certain layer can be approximated by uniformly distributing extra energy to sensor nodes in this layer. The effect of this simplifying assumption will be examined through simulation. Now the original problem can be transformed to determining how to distribute the extra energy in the most efficient way such that the network lifetime can be maximized. Let M denote the total number of available relay nodes, N_l denote the number of sensor nodes in the l^{th} layer, and e_l is the extra energy assigned to each node in the l^{th} layer.

Let R denote the radius of the network and let L denote the total number of layers in the network. For any integers l, k with $0 \leq k < l \leq L$, let $x_{l,k}$ denote

the average number of bits that a node in the l^{th} layer needs to request nodes in the k^{th} layer to forward per unit time. Let g denote the average number of bits each sensor node will generate per unit time. We can readily check that the ratio between the number of nodes in the k^{th} layer and the number of nodes in the l^{th} layer ($k > l$) is $\frac{2k-1}{2l-1}$. Thus the average number of bits that a node in the l^{th} layer will receive from nodes in the k^{th} layer ($k > l$) should be $\frac{2k-1}{2l-1}x_{k,l}$. Let T_{life} denote the network lifetime. Then the original problem can be simplified as follows:

$$\max_{\{x_{i,j},\ e_l\}} T_{life} \quad s.t. \tag{4.3}$$

$$\sum_{k=l+1}^{L} \frac{2k-1}{2l-1} x_{k,l} + g = \sum_{k=0}^{l-1} x_{l,k}, \quad 1 \le l \le L \tag{4.4}$$

$$\sum_{k=0}^{l-1} x_{l,k} P_t(l,k) + \sum_{k=l+1}^{L} x_{k,l} P_r \le \frac{E + e_l}{T_{life}}, \quad 1 \le l \le L \tag{4.5}$$

$$x_{l,k} \ge 0, \quad 0 \le k < l, \quad 1 \le l \le L \tag{4.6}$$

$$\sum_{l=1}^{L} e_l N_l \le M \cdot E, \quad 1 \le l \le L \tag{4.7}$$

$$e_l = \frac{k \cdot E}{N_l}, \quad k \text{ is a non-negative integer}, \quad 1 \le l \le L \tag{4.8}$$

where $P_t(l,k) = P_t((l-k)r_{min})$. Eqn. (4.4) models the traffic conservation, i.e., for each node the amount of transmitted traffic should be equal to the traffic received plus the traffic generated. Eqn. (4.5) poses the energy constraint. Eqn. (4.6) guarantees the feasibility of the solutions and prevents nodes sending traffic further away from the sink. Eqn. (4.7) applies relay nodes quantity constraint. Eqn. (4.8) guarantees the integrity of the relay nodes, that is, the energy of one relay node cannot be split into two parts.

4.2 Numerical Results

This section is devoted to solving the optimization problem defined in Section 4.1 numerically. Since the optimization problem (4.3)-(4.8) is a mixed-integer non-linear programming problem, which is known to be a NP-hard problem, in this work we resort to developing efficient heuristics to solve this problem.

We attack this problem using the following greedy heuristic approach: after sensor nodes have been deployed, relay nodes will be added to the network one by one. Each time when a relay node is added to the network, it will be put in a location that can maximally extend the network lifetime, or more specifically, it will be put in a layer that leads to longest network lifetime. This is motivated by the following observation: due to the asymmetric role of each layer, some layers have utilized energy in a less efficient way by transmitting a large portion of their traffic using a very long range, while some layers have utilized energy in a more efficient way by transmitting most of their traffic with a short range. This indicates that those nodes utilizing energy highly efficiently play a bottleneck role. Here it is worth pointing out that once a new relay is added, the proposed adaptive data propagation scheme in Chapter 3 will be applied to re-calculate the lifetime extension.

Now let us analyze the numerical solutions obtained by the proposed heuristic. To make the results solid, our analysis is based on some typical energy consumption parameters [5, 24]. Specifically, we set $\gamma_1 = 45$nJ/bit, $\gamma_2 = 135$nJ/bit, and $\beta = 10$pJ/bit/m^2 for $\alpha = 2$. For each parameter setting, there exists an optimal transmission range such that the energy consumption per bit per meter can be minimized, which is referred to as the characteristic distance [5]. In our model, as

in Chap. 3, it is easy to check that the characteristic distance d_{char} is:

$$d_{char} = \left(\frac{\gamma_1 + \gamma_2}{\beta(\alpha - 1)} \right)^{\frac{1}{\alpha}}. \tag{4.9}$$

We fix $r_{min} = d_{char}$, which is the layer width. The sensor node density is set to be $\frac{20}{\pi \times d_{char}^2}$, which guarantees the network is 3-connected with probability more than 99.99% [4]. Here we further assume the sensor sense area radius is d_{char}. So the sensor density will guarantee the sensing coverage too.

To demonstrate the network lifetime that can be further extended by applying joint relay deployment and adaptive data propagation, we regard the proposed adaptive data propagation scheme, which allows each sensor to send traffic to multiple destinations in multiple layers to maximize the network lifetime (Chapter 3), as the baseline, and normalize the network lifetime achieved by this baseline scheme as 1. Besides the above proposed greedy heuristics, we have also studied the gain achieved by randomly deploying those relay nodes in the network. Specifically, in this case the extra energy provided by the relay nodes will be distributed uniformly to the sensor nodes.

Fig. 4.1 illustrates the numerical results for different network size with different number of extra relay nodes. Specifically, X-axis denotes the total number of relays that will be put to the network, and Y-axis denotes the normalized network lifetime. The two curves represent the achieved network lifetime by applying two different relay deployment scheme: one is solving the optimization problem (4.3)-(4.8) by the above greedy heuristic and one is deploying the relays randomly. In both schemes, the adaptive data propagation scheme in Chapter 3 has been applied.

Fig. 4.1(a) shows the results for the network with radius $10d_{char}$. That is, there are 10 layers in the network. Based on the network size and sensor node

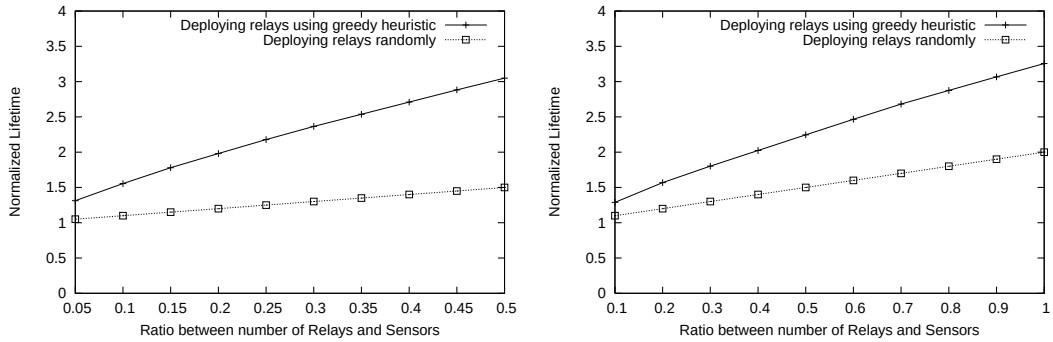

(a) (b)

Figure 4.1: Normalized network lifetime by deploying extra relays (a) 10-layer network (b) 5-layer network

density, it is easy to calculate that there are 2000 sensors in the network. From these results we can see that if we can deploy relays in an effective way, significant gain can be achieved even when only a small number of relays are introduced. For example, when only 10% of extra relay nodes are deployed, the network lifetime can be further extended more than 50% by applying the greedy heuristic deployment method. We can also see that if we deploy nodes randomly, the gain is very minor. For example, adding 1000 relay nodes can only increase the network lifetime by 50% if we deploy them randomly. On the other hand, the network lifetime can be tripled if the 1000 relays are deployed in an efficient way, as demonstrated by the figure.

Fig. 4.1(b) shows the results for a smaller network size. Now we set the network radius to be $5d_{char}$, that is, there are 5 layers in network. From these results we can see that significant network lifetime extension still can be achieved by joint relay deployment and power control. For example, when only 10% of extra relays are added, the network lifetime can be extended by more than 30%. If we compare

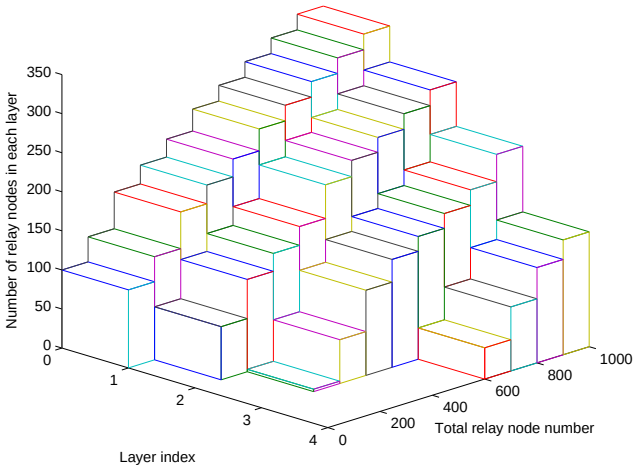

Figure 4.2: The relay nodes distribution in different layers

the results in Fig. 4.1(a) and Fig. 4.1(b), we can see that more network extension can be achieved in a larger network, where 10% extra relays can bring 50% lifetime extension. This is because in larger network, the bottleneck effect around the sink is more significant. This also suggests that the proposed scheme can effectively alleviate the bottleneck effect.

To help better understand the results, we have plotted the relay deployment obtained by the proposed greedy heuristic for the 10-layer network case. The results are illustrated in Fig. 4.2. Given the total number of relay nodes, which is denoted by the total relay node number, this figure plots the number of relay nodes deployed in each layer. For example, when 300 relays will be added, 179 of them will be put into the first (innermost) layer, 118 of them will be put into the second layer, and 3 of them will be put into the third layer. From these results we can see that most relay nodes will be deployed in the inner several layers. For example, even when the number of relays is 1000, there are still no relay nodes that will be deployed to the layers beyond the 4th layer.

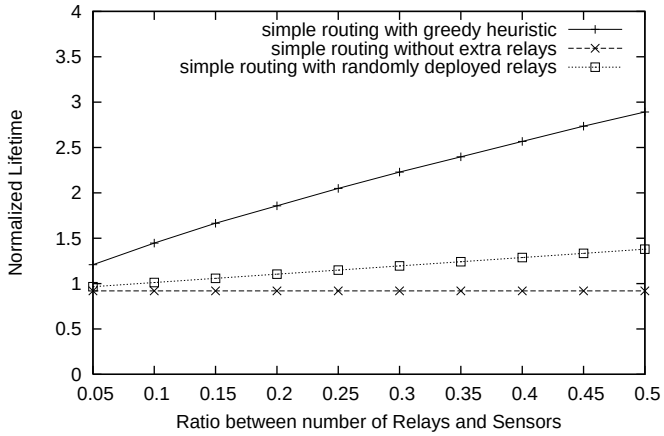

Figure 4.3: Normalized network lifetime by deploying extra relays using simple routing

One problem with the proposed joint node deployment and adaptive data propagation scheme is that it involves a complicated routing scheme. The traffic from one layer may need to be transmitted to several different layers due to the optimality requirement. In previous chapters, we have proposed one simple traffic distribution and power control algorithm: all traffic will be sent to the next inner layer or the sink directly, which is shown to be optimal in some cases and near optimal in the other cases. To make the proposed method more practical, from now on when we do adaptive data propagation, we will adopt this simple strategy. To reflect this change, we modify the original optimization by adding one more constraint: $\{x_{i,j} = 0, j \neq 0 \ \& \ j \neq i-1\}$. Then we can apply the proposed greedy heuristic to re-solve the joint optimization problem.

Fig. 4.3 shows the results for 10-layer network case after applying the modified greedy heuristic. First, from these results we can see that significant gain can still be achieved by the modified scheme, though the modified scheme is much simpler

than the original scheme. For example, when adding 10% extra relay nodes, the network lifetime can still be extended by around 50%. Second, comparing the results in Fig. 4.3 and Fig. 4.1(a), we can see that the modified scheme causes slight performance loss compared with the original case. For example, when 1000 relays are deployed in the network, the network lifetime is extended by 190% instead of 200%. Since the loss is very small, we believe the modified scheme should be adopted when doing joint node deployment and adaptive data propagation due to its simplicity.

4.3 Simulation

This section evaluates the performance of proposed greedy heuristic in randomly deployed sensor network.

The simulation is set up on a randomly deployed circular sensor network with radius $R = 10d_{char}$. The sink is located at the center of the area. For each node (sensor or relay), we set $\gamma_1 = 45$nJ/bit, $\gamma_2 = 135$nJ/bit, $\beta = 10$pJ/bit/m^2 for $\alpha = 2$, therefore $d_{char} \simeq 134m$. The initial energy is 2000 Joule per node. In each unit time (round) each sensor generates a 25-Byte message to be sent to the sink, and relays generate none.

The simulation results are the average from 10 different randomly generated networks. The baseline lifetime is achieved by using simple adaptive data propagation scheme described in Chapter 3 without extra relays. It is worth pointing out that in our simulation, interference has not been considered separately.

In each test, we first randomly deploy the sensor nodes into the network according to the uniform distribution with density $\frac{20}{\pi d_{char}^2}$. We then randomly deploy the relays in layers according to the numerical results from Section 4.2. During

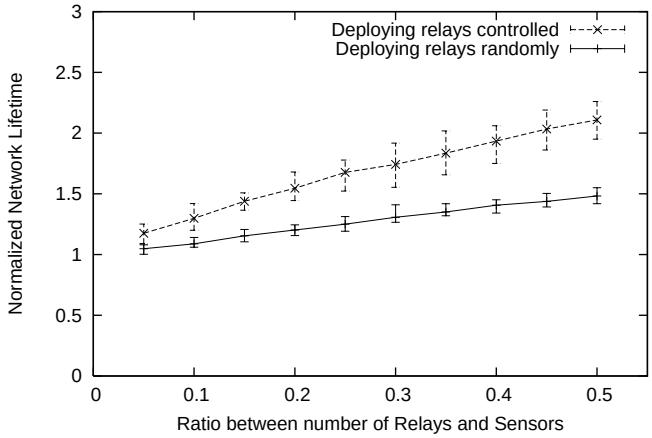

Figure 4.4: Normalized network lifetime by deploying extra relays using simple routing

test, each node transmits its traffic either to the sink or its neighbors which are around d_{char} away.

The simulation results are illustrated in Fig. 4.4. From the results we can see that the proposed scheme brings considerable performance gain. For example, when 10% relay nodes are added into the network strategically, around 35% lifetime extension can be obtained. The results also show the same trend as the numerical results (Fig. 4.3), but with lower lifetime extension. This is because when we model the problem into the joint optimization problem (4.3)-(4.8), we make an approximation that adding relay nodes into the network is equivalent to adding energy to the sensor nodes. In real network, when a sensor runs out of energy, the network will lose the coverage and then the network will terminate; however, the relay nodes may still have considerable energy left. In this situation, adding relay nodes into the network is actually not equivalent to adding energy to the sensor nodes. So this approximation leads to the gap between numerical results

and simulation results.

4.4 Summary

Battery powered wireless sensor network is extremely energy constrained. The all-to-one communication pattern in general homogeneous sensor networks makes the sensors around the sink deplete the energy much faster than faraway sensors due to the heavily relay burden. To conquer this problem, various schemes are proposed. In this paper we solve this problem by joint relay deployment and adaptive data propagation scheme. We model the problem as a mixed-integer nonlinear programming problem, which is known to be NP-hard. We then solve the optimization problem using greedy heuristic which is verified to be effective by both numerical results and simulation results.

Chapter 5

Fault Tolerance and Attack Resilience Measurement of Wireless Ad Hoc Networks

In the first part of this dissertation (Chapter 2, Chapter 3 and Chapter 4) we have studied how to maximally extend the lifetime of randomly deployed wireless sensor networks by adaptive traffic distribution and power control. In this chapter we will study another important issue in randomly deployed wireless ad hoc networks: fault tolerance and attack resilience measurement. The rest of this chapter is organized as follows. Section 5.1 introduces the network model and the metrics. Section 5.2 investigates the properties of the pairwise connectivity for Poisson and geometric random graphs. The network fault tolerance is studied in Section 5.3, and the attack resilience is studied in Section 5.4. Finally, Section 5.5 summarizes this chapter.

5.1 Network Models and Metric Definitions

In this section, we first introduce the random graph models used to model the wireless ad hoc networks, then describe the different connectivity definitions as well as α-p-resilience, and finally compare pairwise connectivity with network connectivity.

5.1.1 Network Modeling

In the literature, random graphs have been widely used to model various networks [4, 6, 35, 46]. In order to model wireless ad hoc networks, Poisson random graphs have been suggested by [14]. However, since Poisson random graphs do not consider correlations between different links, in many situations it may not be the best model. To fix this problem, a modified version of Poisson random graphs, geometric random graphs, have been widely used recently [4]. In this work, both models will be studied, though the geometric random graph model will be the focus.

Poisson Random Graphs

After being independently proposed by [55], and [21, 22], Poisson random graphs have been widely applied to model various networks [6], and have been well studied by mathematicians, and many results, both approximate and exact, have been proved [7, 44]. In general, a *Poisson random graph* $G(N, p)$ is a graph with N nodes in which for each pair of nodes, with probability p there is an edge between them. By holding the average node degree $\lambda = p(N-1)$ constant, the probability of a node having degree k can be calculated as

$$p_k = \binom{N-1}{k} p^k (1-p)^{N-1-k} \simeq \frac{e^{-\lambda}\lambda^k}{k!}, \tag{5.1}$$

with the last approximate equality becomes exact in the limit of large N and fixed k, from which the name "Poisson random graph" comes.

Geometric random graph

In the literature, geometric random graphs have also been widely used to model various ad hoc wireless networks [4, 35, 46]. Since the construction of geometric random graphs has incorporated the spatial correlations between nodes and edges, it can better model the topologies of wireless ad hoc networks. In this work we will mainly focus on the two-dimensional case, where now a *geometric random graph* $G(N, r)$ is a graph in which N nodes are independently deployed inside a large area of size A according to the 2D uniform distribution[1], and for any pair of nodes there exists an edge between these two nodes if and only if the distance between them is no more than r (e.g., in wireless ad hoc networks, r is nodes' maximum transmission range). Let $\gamma = \frac{N\pi r^2}{A}$ denote the *normalized average node density* of such a random graph, which denotes the average number of nodes inside a circle with radius being r. In this work, we simply refer to normalized average node density as average node density. For any node not lying in the boundary area[2] of the network deployment, the probability of a node having degree k can be calculated as

$$p_k = \binom{N-1}{k} \left(\frac{\pi r^2}{A}\right)^k \left(1 - \frac{\pi r^2}{A}\right)^{N-1-k} \simeq \frac{e^{-\gamma}\gamma^k}{k!}, \tag{5.2}$$

[1]A node v is deployed inside an area A according to the 2D uniform distribution if for any subarea $A_1 \subset A$, $P(v \in A_1 | v \in A, A_1 \subset A) = A_1/A$.

[2]In this work, we say a node v lies in the boundary area of a network deployment if and only if there exists at least one location which does not lie in the deployment area and whose distance to node v is less than r

with the last approximate equality becomes exact in the limit of large A and N and fixed k. That is, the distribution of degree also follows Poisson distribution with the average degree being γ. It is worth mentioning that due to the boundary effects (e.g., the average degree of nodes inside the boundary area is less than the average degree of nodes not inside the boundary area), the average node degree of a geometric random graph is less than its average node density.

5.1.2 Pairwise Connectivity and α-p-resilience

Based on the above network models, a wireless ad hoc network can be represented as an undirected graph $G = G(V, E)$ at each time instant, which comprises $|V|$ nodes and $|E|$ edges, and for any $u, v \in V$, if $(u, v) \in E$, then $(v, u) \in E$. Two nodes u and v are said to be connected if there exists at least one path between u and v; otherwise these two nodes are said to be disconnected. Given any pair of nodes $u, v \in V$, let $C(u, v)$ denote the maximum number of node-disjoint paths[3] from node u to node v, which we refer to as the *pairwise connectivity* of node pair (u, v). Equivalently, $C(u, v) = k$ means that there exist no such set of $k-1$ nodes whose removal would make u and v disconnected, and there exists at least one set of k nodes whose removal would make u and v disconnected. A node pair (u, v) is said to be k-pairwise-connected if $C(u, v) \geq k$. Since G is undirected, we always have $C(u, v) = C(v, u)$.

According to [6], a graph $G = G(V, E)$ is said to be connected if any pair of nodes in G is connected, and G is said to be k-connected if for any pair of nodes $u, v \in V$, $C(u, v) \geq k$. It is easy to see that this measure focuses on

[3]A set of paths from u to v are said to be node-disjoint if these paths do not share any common nodes except u and v.

the worst case scenario. However, in many situations, even if the network becomes disconnected, i.e., some nodes become isolated, the remaining nodes in the network can still communicate with each other with very high probability. For example, in a self-organized wireless ad hoc network [68], individual nodes are only interested in whether their own communication request can be satisfied, and in general a single node isolated from the network will not significantly affect the other nodes, although the network is disconnected.

In order to measure the average case network service availability, we introduce the following metrics: *average pairwise connectivity* and *pairwise connected ratio*. For any graph G, the average pairwise connectivity (APC) of G, denoted by $C(G)$, is defined as follows:

$$C(G) = \frac{1}{N(N-1)} \sum_{u \in V} \sum_{v \neq u \in V} C(u, v), \tag{5.3}$$

which is the average number of node-disjoint paths between any pair of nodes in the network. Similarly, pairwise connected ratio (PCR) is defined as follows:

$$PCR(G) = \frac{1}{N(N-1)} \sum_{u \in V} \sum_{v \neq u \in V} \mathbf{1}[C(u, v) \geq 1], \tag{5.4}$$

which is the indicator version of APC. It is the proportion of node pairs that are pairwise connected, i.e., can communicate with each other. In other words, from an individual node's point of view, this is the proportion of nodes in average that it can reach in the network. Meanwhile, a network with PCR being α indicates that there exists at least one connected component which comprises at least α portion of the total nodes.

In general, fault tolerance or attack resilience can be measured as the decrease of network performance due to node or edge removal. In this chapter we propose α-p-resilience to measure the decrease of network service availability under node

removal. Specifically, given a network G, if it is α-p-resilient in PCR, then even after removing p portion of nodes, the PCR is still no less than α, that is, for any remaining node in the network, it can still expect to connect to α portion of the remaining nodes. Similarly, given a network G, if it is α-p-resilient in APC, then even after removing p portion of nodes, the APC is still no less than α, that is, the average number of node-disjoint paths between any pair of remaining nodes is at least α.

5.1.3 Pairwise Connectivity vs. Network Connectivity

In this subsection we study the difference between pairwise connectivity and network connectivity through experiments. In the experiments, a set of geometric random graphs are generated with the deployment areas varying from $10r \times 10r$ to $50r \times 50r$, where r is node's transmission range. The PCR and network connected ratio (NCR) for different network size and node density are illustrated in Fig. 5.1, where NCR denotes the percentage of connected networks among all the generated networks. In Fig. 5.1 each data point is the average result over 1000 independently generated random graphs.

First, from these results we can see that although in many situations the network connected ratio is low, that is, a large portion of the generated networks are not connected, almost all pairs of nodes in the network can communicate with each other. For example, for the network size being $20r \times 20r$ and node density being 10, which can be a very reasonable configuration for a wireless ad hoc network, only about 14% of the generated networks are connected, while more than 99.9% of node pairs in the generated networks can communicate with each other through one or more routes. This suggests that in many situations network connectivity

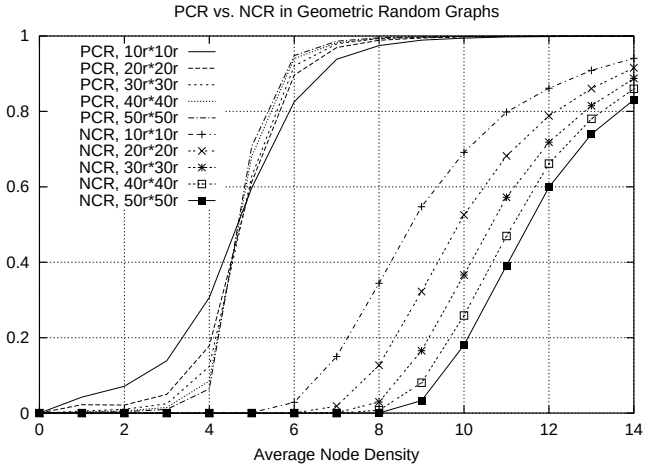

Figure 5.1: Comparison between pairwise connected ratio and network connected ratio

may not be an appropriate metric to measure the average case network service availability.

Second, by comparing the NCR values illustrated in Fig. 5.1 under different network configuration, we can see that with the increase of network size, the network connected ratio will decrease, which is easy to understand: the more the number of nodes in the network, the higher the probability that some nodes will become isolated. However, from Fig. 5.1 it is surprising to see that whenever the node density is no less than 5, by fixing the node density, the larger the network size, the higher the PCR, although more nodes will become isolated. That indicates that the more the number of nodes in the network, usually the better the service availability that the network may provide, since each node may have more resources to use and more options to take. This also suggests that network connectivity may not be appropriate when used to measure the network service availability.

Third, from these results we can see that the PCR curves exhibit sharp thresh-

old behaviors, where the PCR increases dramatically when the node density increases from 4 to 6. With node density 4 the PCR is less than 20% for most cases, while with node density 6 the PCR becomes more than 90% in most cases. Furthermore, all these PCR curves intersect with each other at around density 5. When the node density is less than 5, the larger the network, the lower the PCR; while when the node density is greater than 5, the larger the network, the higher the PCR. This is the combined effect of path length and available resources: the longer the path length, the lower the probability that a pair of nodes can connect; while the more the resources, the higher the probability that a pair of nodes can connect. When node density is very low, the effect of path length will dominate the effect of available resources (the average path length in the networks with size $10r \times 10r$ is only about half of that in the networks with size $20r \times 20r$). When the node density becomes high, the effect of available resources will play a dominant role.

Finally, from these results we can see that to maintain high pairwise connectivity, the node density should be no less than 7. From the results in this figure we can see that when the density is less than 7, in all five cases the PCR is less than 95%. The network size may affect this threshold, but not significantly. Meanwhile, we can see that when the node density is larger than a certain value (e.g., 10), the PCR will closely approach 1. In other words, as long as the node density is higher than some threshold, a certain level of service availability can be guaranteed.

5.2 The Pairwise Connectivity of Wireless Ad hoc Networks

In this section we focus on studying the service availability of wireless ad hoc networks based on the following two metrics: APC and PCR. When studying the APC, we have derived an analytical upper-bound for APC, and demonstrated that the APC can be approximated by its upper-bound very well for Poisson random graphs and for the inner part of geometric random graphs.

Given any graph $G(V, E)$ and any node $u \in V$, let $d(u)$ denote the degree of node u, that is, the number of neighbors of node u. Then for any pair of nodes $u, v \in V$, let

$$C_{upper}(u, v) = \min\{d(u), d(v)\}. \tag{5.5}$$

Since it is obvious that the number of node-disjoint paths between u and v cannot exceed the degrees of u and v, $C_{upper}(u, v)$ is always an upper bound of $C(u, v)$. Accordingly, we can define the upper bound of $C(G)$ as follows:

$$C_{upper}(G) = \frac{1}{N(N-1)} \sum_{u \in V} \sum_{v \neq u \in V} C_{upper}(u, v). \tag{5.6}$$

For any graph $G(V, E)$ and any pair of nodes $u, v \in V$, let $d_{diff}(u, v)$ denote the difference between $C_{upper}(u, v)$ and $C(u, v)$, that is,

$$d_{diff}(u, v) = C_{upper}(u, v) - C(u, v). \tag{5.7}$$

Let d_{diff} denote the random variable representing the difference between the upper bound and exact value of any pair of nodes in the network. In other words, given a graph, d_{diff} corresponds to picking a pair of nodes (u, v) at random and taking $d_{diff}(u, v)$. Then for any pair of nodes, the probability that the difference between

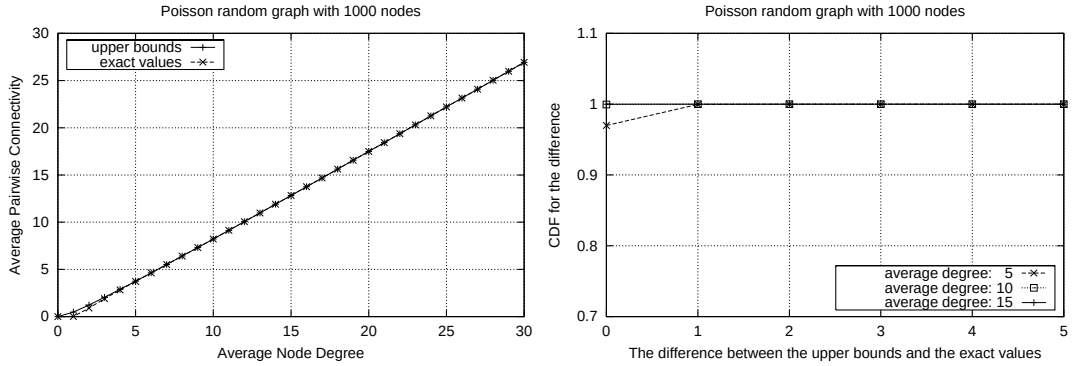

(a) (b)

Figure 5.2: Upper bounds and exact values of APC for Poisson random graphs

their upper bound of pairwise connectivity and the exact pairwise connectivity is equal to k can be calculated as follows:

$$P(d_{diff} = k) = \sum_{u \in V} \sum_{v \neq u \in V} \frac{\mathbf{1}[d_{diff}(u, v) = k]}{N(N-1)}, \tag{5.8}$$

where $\mathbf{1}[condition]$ is an indicator function defined as follows:

$$\mathbf{1}[condition] = \begin{cases} 1 & condition \text{ is true} \\ 0 & condition \text{ is false} \end{cases} \tag{5.9}$$

5.2.1 Poisson Random Graphs

We first study the APC in Poisson random graphs through experiments, which are set up as follows: the total number of nodes, denoted by N, is fixed to be 1000, and for any pair of nodes, with probability p there is an edge to directly connect them. Different values of p are tested, and the average node degree can be calculated as $(N-1)p$. The experimental results with different average node degrees are shown in Fig. 5.2, where Fig. 5.2(a) illustrates the relationship between the average node degree and the APC (both $C_{upper}(G)$ and $C(G)$ are shown), and

Fig. 5.2(b) demonstrates the distribution of D_{diff}, the difference between the upper bound and exact value of the APC, under three different average node degrees: 5, 10, and 15. For each average node degree, the results are averaged over 1000 independently generated Poisson random graphs.

First, from these results we can see that the APC increases monotonically with the increase of average node degree, which is easy to understand. Second, it is surprising to see that the upper bounds and exact values of the APC are almost equal in all configurations, except when the average node degree is extremely low (e.g., average node degree is less than 5), which indicates that the APC of Poisson random graphs can be almost completely characterized by the corresponding upper bounds. These results also indicate that in Poisson random graphs, when the average node degree is large, the bottleneck to find multiple node-disjoint paths between a pair of nodes lies in the degrees of the two nodes themselves.

Now we show how to directly calculate the upper bound of APC for Poisson random graphs. Here we make the simplifying assumption that the degree distributions for different nodes are independent in Poisson random graphs, though it may not be strictly true. When N is large and $(N-1)p = \lambda$, given any pair of nodes u and v, it is easy to show that the probability of $C_{upper}(u,v)$ equal to k can be calculated as follows:

$$\begin{aligned} & P(C_{upper}(u,v) = k) \\ = \; & P(d(u) = k)P(d(v) > k) + P(d(u) \geq k)P(d(v) = k) \\ = \; & \frac{e^{-\lambda}\lambda^k}{k!}\left(\sum_{i=k+1}^{\infty}\frac{e^{-\lambda}\lambda^i}{i!} + \sum_{i=k}^{\infty}\frac{e^{-\lambda}\lambda^i}{i!}\right) \end{aligned} \tag{5.10}$$

Under the simplifying assumption of independence, according to the Strong Law of Large Numbers [31], for large N, $C_{upper}(G)$ is approximately equal to $E[C_{upper}(u,v)]$,

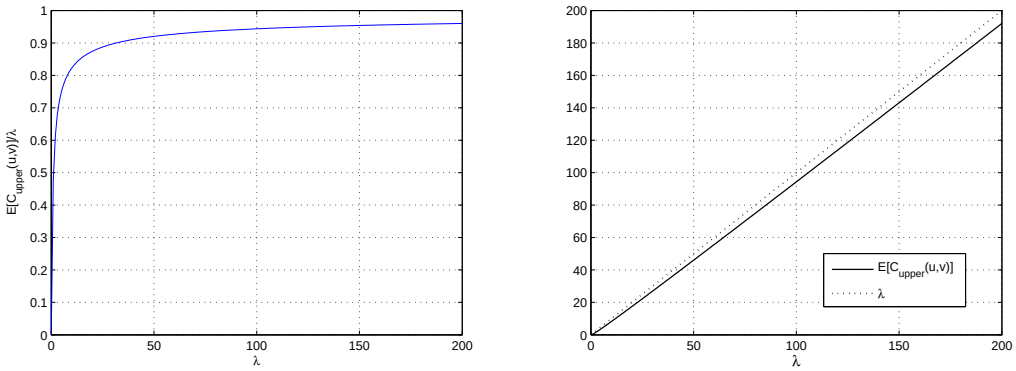

(a) (b)

Figure 5.3: Relationship between $E[C_{upper}(u,v)]$ and λ

where $E[C_{upper}(u,v)]$ can be calculated as follows:

$$\begin{aligned} & E[C_{upper}(u,v)] \\ = & \sum_{k=0}^{\infty} k \frac{e^{-\lambda}\lambda^k}{k!} \left(1 - \sum_{i=0}^{k} \frac{e^{-\lambda}\lambda^i}{i!} + \sum_{i=k}^{\infty} \frac{e^{-\lambda}\lambda^i}{i!}\right) \\ = & \lambda - \lambda \left(\sum_{k=0}^{\infty} \frac{e^{-\lambda}\lambda^k}{k!} \sum_{i=0}^{k+1} \frac{e^{-\lambda}\lambda^i}{i!} - \sum_{k=0}^{\infty} \frac{e^{-\lambda}\lambda^k}{k!} \sum_{i=k+1}^{\infty} \frac{e^{-\lambda}\lambda^i}{i!}\right) \\ = & \lambda - \lambda \sum_{k=0}^{\infty} \frac{e^{-\lambda}\lambda^k}{k!} \left(\frac{e^{-\lambda}\lambda^k}{k!} + \frac{e^{-\lambda}\lambda^{k+1}}{(k+1)!}\right) \end{aligned} \tag{5.11}$$

Since there is no closed form for (5.11), next we study the relationship between $E[C_{upper}(u,v)]$ and the average node density λ by truncating the equation at $k = 2000$. Fig. 5.3 illustrates the computed results based on Eqn. (5.11). Fig. 5.3(a) illustrates the ratio between $E[C_{upper}(u,v)]$ and λ, which demonstrates that the ratio increases fast when λ is small, then increases slowly. Fig. 5.3(b) illustrates the values of $E[C_{upper}(u,v)]$ for different average node degrees, which indicates that although the ratio is not constant, $E[C_{upper}(u,v)]$ is approximately a linear function of the average node degree. This is also consistent with the experimental findings illustrated in Fig. 5.2(a). From Fig. 5.3(b) we can also see that the absolute

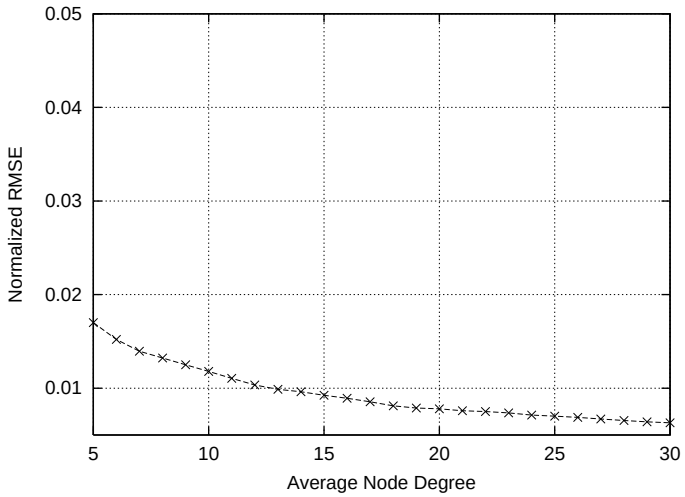

Figure 5.4: Relationship between normalized RMSE and average node degree

difference between $E[C_{upper}(u,v)]$ and λ will increase with the increase of λ, which indicates that the ratio can never be equal to 1.

It is easy to check that $E[C_{upper}(u,v)]$ is an unbiased estimator for $C_{upper}(G)$. Now we study the normalized root mean square error (NRMSE) associated with the estimator $E[C_{upper}(u,v)]$, which is defined as

$$NRMSE = \frac{\sqrt{E\big[(E[C_{upper}(u,v)] - C_{upper}(G))^2\big]}}{E[C_{upper}(u,v)]}.$$

The experimental results are illustrated in Fig. 5.4, which are based on 1000 independently generated Poisson random graphs. From these results we can see that the normalized RMSE is very small and decreases with the increase of average node degree, so $C_{upper}(u,v)$ is well-approximated by its mean value $E[C_{upper}(u,v)]$.

5.2.2 Geometric Random Graphs

Now we study the pairwise connectivity in geometric random graphs. In this set of experiments, the geometric random graphs are generated as follows: nodes are

independently deployed inside a rectangular area of $10r \times 10r$ according to the 2D uniform distribution, and the total number of nodes in the network changes with the change of average node density. The experimental results with different average node densities are illustrated in Fig. 5.5, where Fig. 5.5(a) shows the relationship between the average node density and the sample mean of APC (both $C_{upper}(G)$ and $C(G)$ are shown), Fig. 5.5(b) demonstrates the distribution of d_{diff}, that is, the difference between the upper bound and exact value of the APC, under three different average node densities: 10, 20, and 30, and Fig. 5.5(c) exhibits the standard deviation of APC. Similar to the case of Poisson random graphs, for each average node degree, the results are averaged over 1000 independently generated geometric random graphs.

First, from Fig. 5.5(a) we can see that the APC increases with the increase of node density, which is easy to understand. Second, unlike in Fig. 5.2(a) (Poisson random graphs), the upper bounds and exact values of the APC are not approximately equal in the Fig. 5.5(a) (geometric random graphs). The distributions of d_{diff} are illustrated in Fig. 5.5(b), which shows that the difference between the upper bounds and exact values can become large in certain situations. For example, for average node density 10, with probability only 20% the upper bounds are equal to the exact values. Further, for all the three node densities shown in Fig. 5.5(b), with about probability of 15% the difference is larger than 3. The standard deviations exhibited in Fig. 5.5(c) show that when the average node density is larger than 7, the standard deviation becomes negligible. In other words, for any arbitrary geometric random graph generated according to the above procedure, its actual APC can be approximated by the sample mean (illustrated in Fig. 5.5(a)) very well.

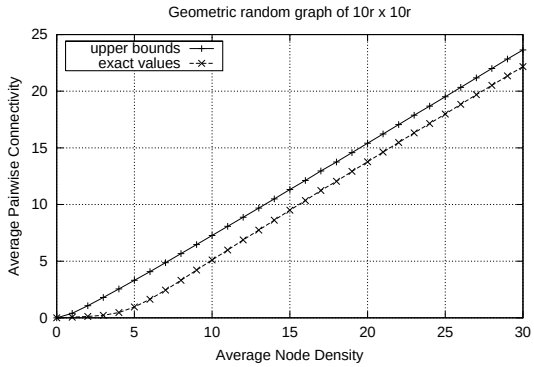

(a)

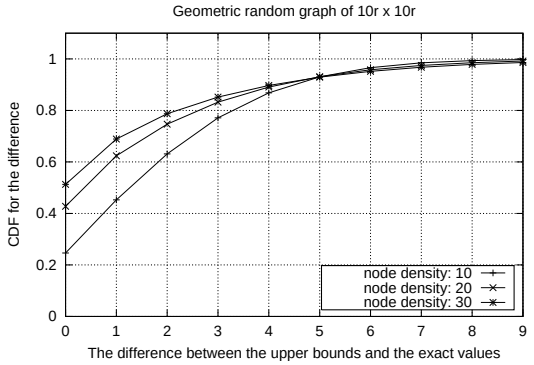

(b)

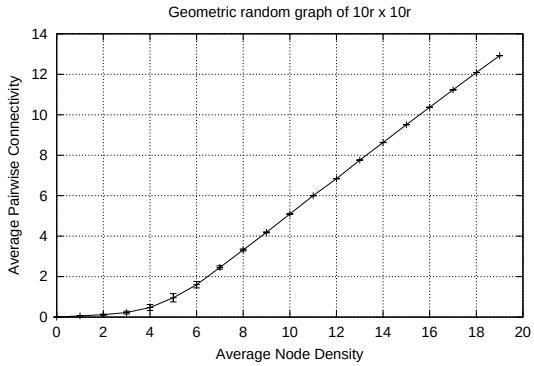

(c)

Figure 5.5: Upper bounds and exact values of APC in geometric random graphs

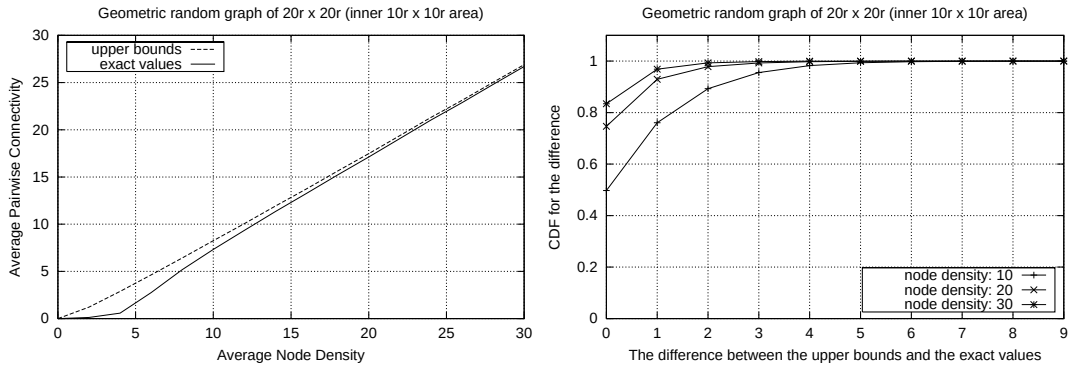

(a) (b)

Figure 5.6: Upper bounds and exact values of APC in the inner part of geometric random graphs

One possible reason for the existence of a gap between the upper bounds and the exact values is the existence of boundary effects and the non-homogeneity of geometric random graphs. Unlike Poisson random graphs, in which all nodes are homogeneous and there is no such concept of boundary, in geometric random graphs, some nodes may lie in the boundary areas and may have less resources when trying to discover routes to the other nodes, which can greatly reduce the pairwise connectivity.

To investigate the boundary effects in geometric random graphs, we have conducted another set of experiments, where only nodes inside the inner area of geometric random graphs are considered when calculating the APC. Specifically, given a geometric random graph in a rectangular area of $20r \times 20r$, only node pairs with both inside the inner area of $10r \times 10r$ are considered. The new experimental results are illustrated in Fig. 5.6. From these results we can see that with the increase of node density, the exact values of the APC are almost equal to the upper bounds. Meanwhile, the distribution of the difference between the upper bound

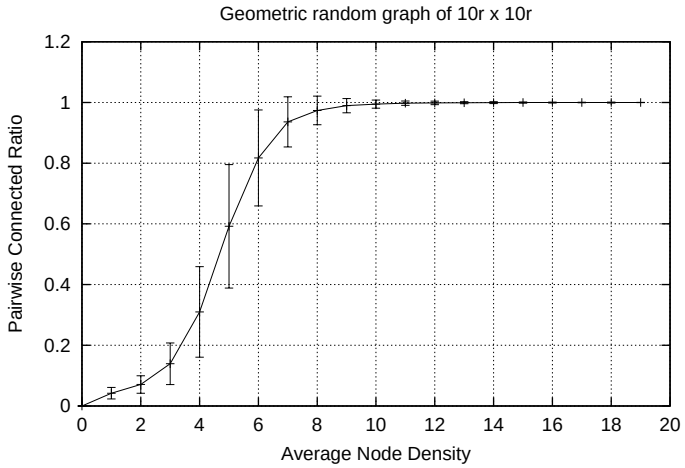

Figure 5.7: Sample mean and standard deviation for PCR in geometric random graph

and exact value also demonstrates that the differences become much smaller than the results shown in Fig. 5.5(b), and with only very small probability the gap is larger than 3. In other words, when the boundary effects are removed and the node density is not too low, the pairwise connectivity of each node pair can be completely characterized by their own node degrees.

The PCR in geometric random graphs has also been studied with the same configuration, where the results are illustrated in Fig. 5.5. The sample mean and standard deviation of PCR are illustrated in Fig. 5.7. Except for the sharp threshold behavior, which has been illustrated in Section 5.1(C), from these results we can also see that the standard deviation becomes very small when the average node density becomes large (i.e., PCR approaches to 1). This indicates that for an arbitrary geometric random graph with large average node density (e.g., larger than 10), with very high probability nearly every pair of nodes can communicate, though the network may be disconnected.

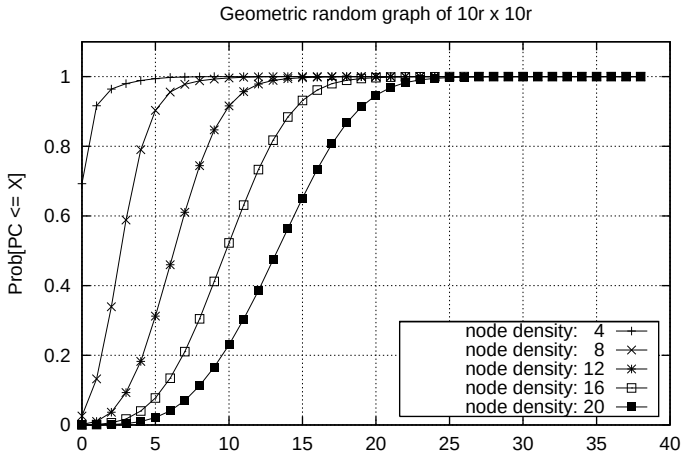

Figure 5.8: Distribution of Pairwise Connectivity

5.2.3 Distribution of Pairwise Connectivity

We have also conducted a set of experiments to further study the distribution of pairwise connectivity in geometric random graphs, and the results are illustrated in Fig. 5.8. In this set of experiments, the network deployment area is fixed to be $10r \times 10r$, and for each node density, the results are averaged over 1000 independently generated random graphs. For each curve in Fig. 5.8, each data point denotes the total fraction of node pairs whose pairwise connectivity is no more than certain value (i.e., x-axis value). Based on these results, we can not only calculate the APC, but also find the distribution of node pairs with different pairwise connectivity.

First, comparing the results in Fig. 5.8 and Fig. 5.5 we can see that the average values match the median values very well. For example, as illustrated in Fig. 5.5, the APC for node density 20 is about 13, while as shown in Fig. 5.8, the median point corresponding to node density 20 is also around 13. This is also true for other node densities. This is because the pairwise connectivity for different nodes pairs is distributed almost uniformly in a small region and centered at their median

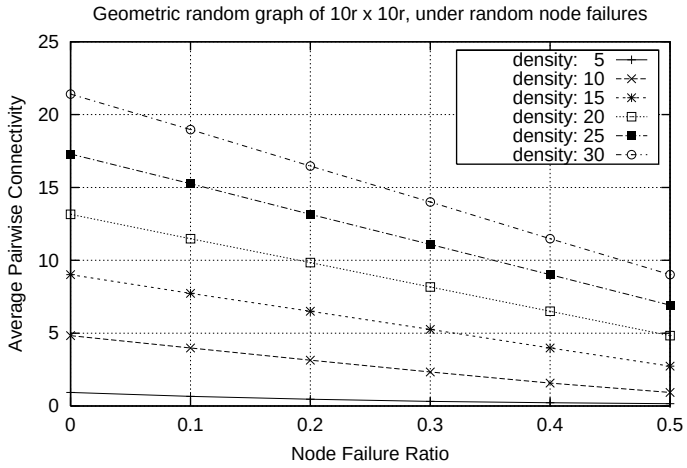

Figure 5.9: The α-p-resilience in APC for geometric random graphs under random node failures

point. Second, from the results illustrated in Fig. 5.8 we can see that these curves exhibit some threshold behaviors where the curves change sharply from 0 to 1 for most node densities. That is, with very high probability most node pairs' pairwise connectivity is around the APC, which also shows that APC can be a very good metric from each individual node's point of view.

5.3 Experimental Evaluation of Fault Tolerance

In wireless ad hoc networks, some nodes may be removed from the network due to exhaustion of battery power and some nodes may be disconnected from the network due to unintentional configuration errors. Meanwhile, due to the fragile wireless connections and possible mobility, link breakage may happen very frequently. The measure of fault tolerance is thus critical in wireless ad hoc networks. In this section, we study the fault tolerance of such networks under random node failures based on the proposed α-p-resilience measure, where both APC and PCR have

been studied.

We first conduct a set of experiments to study the decrease of APC in geometric random graphs under random node failures. In this set of experiments, the initial network is deployed in a rectangular area of $10r \times 10r$, and the average node density ranges from 5 to 30. The experimental results are illustrated in Fig. 5.9, where each data point represents the APC after a portion of nodes are randomly removed from the network, which corresponds to random node failure with certain failure ratio, and are obtained through averaging over 1000 independently generated geometric random graphs. In other words, for any point (x, y) in the curve corresponding to the original average node density γ, this indicates that the above geometric random network with average node density γ is y-x-resilient in APC. From these results we can see that the APC decreases linearly with the increase of node failure ratio. The results also confirm that the random failure of nodes with failure ratio p has exactly the same effect as reducing the node density to $1 - p$ of the original density, which is trivial to understand.

The experimental studies of α-p-resilience in PCR for geometric random graphs are illustrated in Fig. 5.10, where the same experiment configurations are used as in Fig. 5.9. In this figure, each curve corresponds to a specific PCR (that is, α) under certain portion of random node removal. For example, for the point (8, 0.3) in the curve corresponding to PCR = 99%, this indicates that a network with APC being 8 is 99%-30%-resilient under random node failure, i.e., up to 30% of the nodes can be randomly failed while maintaining a PCR of at least 99%. From these results we can see that the network resilience increases with the increase of APC, which is trivial to understand. These results also demonstrate that the extra portion nodes that can be removed when decreasing the PCR from 99% to 95% is

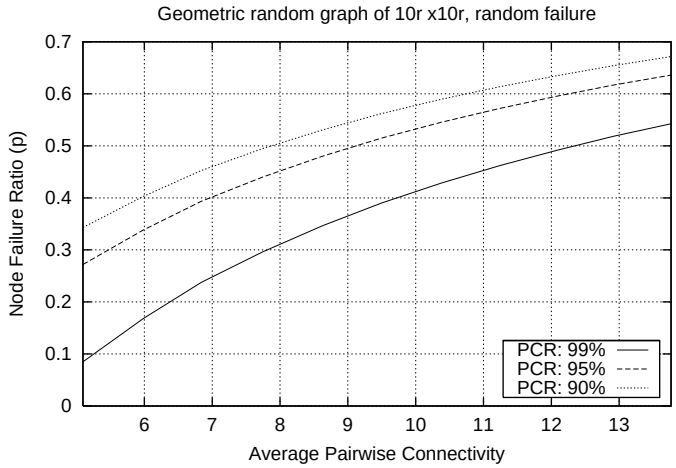

Figure 5.10: The α-p-resilience in PCR for geometric random graphs under random node failures

much larger than that when decreasing the PCR from 95% to 90%. This can be explained by the sharp threshold behavior: according to the results illustrated in Fig. 5.7, with the decrease of average node density, the decrease of PCR from 95% to 90% is much quicker than the decrease of PCR from 99% to 95%.

Random failure experiments have also been conducted on Poisson random graphs, and the results are illustrated in Fig. 5.11. In this set of experiments, there are 1000 nodes in the initial deployment of each network, and the average node degree ranges from 5 to 30. The results confirm that the random failure of nodes with failure ratio p has exactly the same effect as reducing the average node degree to $1 - p$ of the original average node degree.

5.4 Experimental Evaluation of Attack Resilience

This section evaluates the attack resilience of wireless ad hoc networks based on the metric of α-p-resilience. In many situations the networks are deployed in ad-

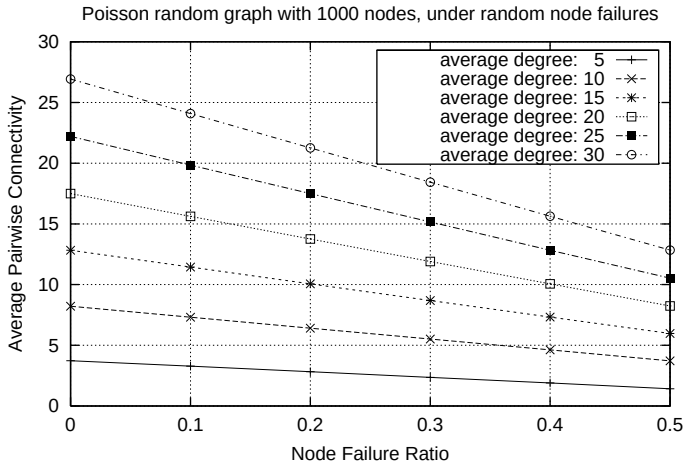

Figure 5.11: The α-p-resilience in APC for Poisson random graphs under random node failures

versarial environments, and some nodes may become dysfunctional under attacks. Thus the study of attack resilience is also critical. In this section, the following two attack models are considered: selective node removal attacks according to node degree and partition attacks.

When selective node removal attacks are applied, nodes in the network are removed one by one, and at each step the node with the highest degree is removed. This type of attack can degrade the network performance drastically in scale-free networks, such as the Internet [2]. However, since randomly deployed wireless ad hoc networks are not scale-free, selective node removal attacks may not be the best attack model from the attackers' point of view. In this section, we also consider another type of attack whose goal is to partition the network into many disconnected components through removal of nodes in certain areas. We refer to this type of node removal attacks as partition attacks.

Fig. 5.12 shows the experimental results of α-p-resilience for Poisson random graphs under selective node removal attacks, or more specifically, the decrease of

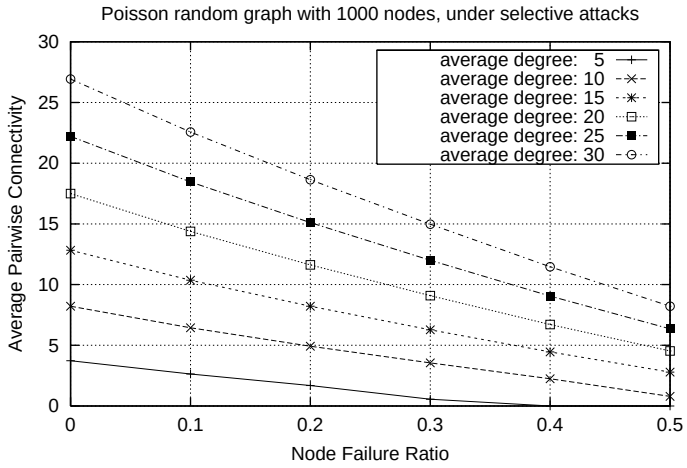

Figure 5.12: The α-p-resilience in APC for Poisson random graphs under selective node removal attacks

APC with the increase of node removal fraction for a given network configuration. In this set of experiments, the original number of nodes in the network is set to be 1000, the average node degree varies from 5 to 30. Each data point in this figure corresponds to the APC under the selective removal of a certain fraction of nodes, The result is obtained through 1000 independently generated Poisson random graphs. From these results we can see that the APC decreases approximately linearly with the increase of node removal percentage, similar to the case of random node failure shown in Fig. 5.11.

The comparisons between random node removal and selective node removal have also been performed, as illustrated in Fig. 5.13. From these comparisons we can see that although in both cases the APC will approximately decrease linearly with the increase of node removal fraction, selective node removal can cause more degradation than random node removal. Meanwhile, even under selective node removal attacks, the APC in Poisson random graphs still decreases very gracefully, which indicates that Poisson random graphs are robust to selective node removal

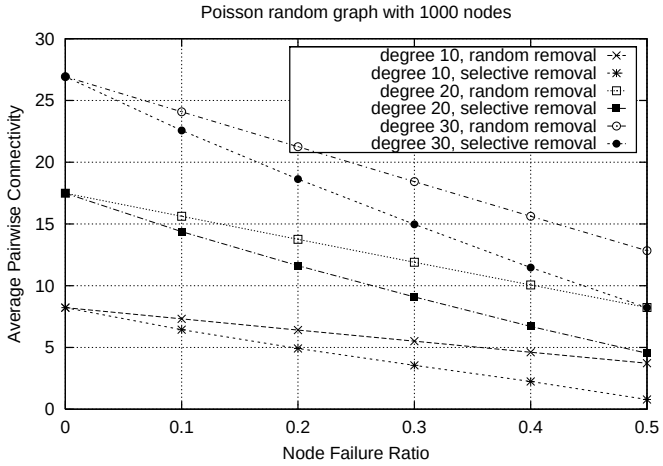

Figure 5.13: Comparison of APC for Poisson random graphs under different attacks

attacks.

Since geometric random graphs can better capture the spatial correlation among nodes in wireless ad hoc networks, in the remainder of this section we will focus on geometric random graphs. Further, besides selective node removal attacks, the effect of partition attacks will be studied. Fig. 5.14 illustrates the experimental results for geometric random graphs. In this set of experiments, the network deployment area is fixed to be $10r \times 10r$, the original node density ranges from 5 to 30, and the fraction of nodes removed varies from 10% to 50%.

From the results illustrated in Fig. 5.14(a), which correspond to the case of selective node removal attacks, we can see that the APC decreases linearly and gracefully with the increase of node removal percentage, similar to the case of Poisson random graphs shown in Fig. 5.12. This also indicates that geometric random graphs are robust to selective node removal attacks unless the node density is too low, although the selective node removal attacks may cause more damage than the random node failures.

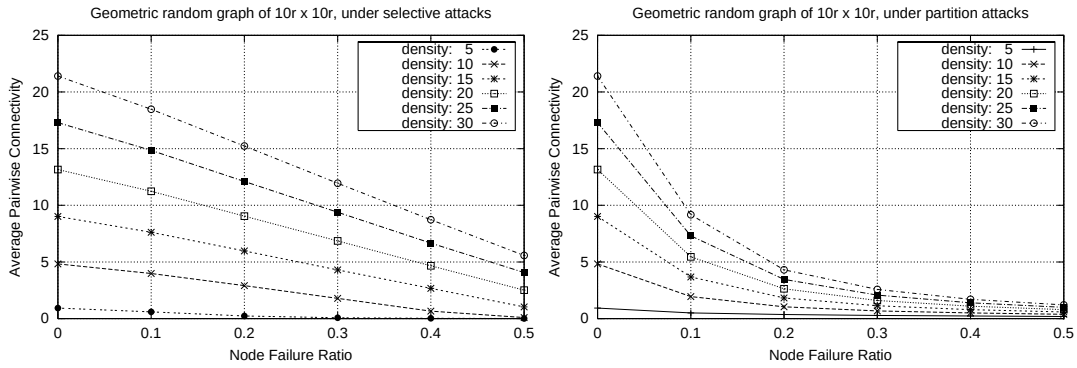

Figure 5.14: The α-β-resilience in APC for geometric random graphs under selective node removal and partition attacks

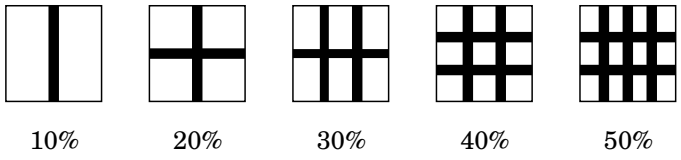

Figure 5.15: Partition methods for different node removal ratios. In these figures, the dark areas denote those areas from which all nodes have been removed, and the width of each dark area is at least r.

Now we study the effects of partition attacks, where the partition strategies are illustrated in Fig. 5.15. From the experimental results presented in Fig. 5.14(b) we can see that partition attacks can cause severe performance degradation in geometric random graphs. For example, when only 10% of nodes are removed, the APC will decrease to about 40% of the original value. This makes sense since according to the partition strategy shown in Fig. 5.15, after 10% of nodes are removed, the network will be partitioned into two disconnected parts. In other words, for any node in the network, it will lose connection to about half of the nodes in the network. Further, due to the reduction of available resources and

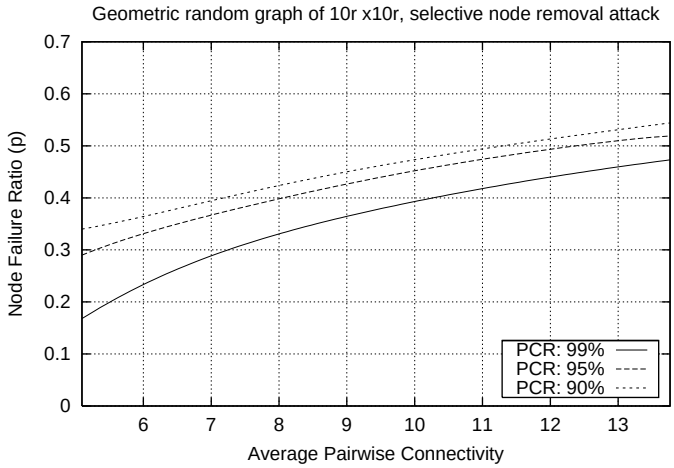

Figure 5.16: The α-p-resilience in PCR for geometric random graphs under selective node removal attacks

network size, the number of node-disjoint paths between pairs of nodes that remain connected also decreases, which explains why the obtained APC is only about 40% of the original value.

Fig. 5.16 demonstrates the α-p-resilience in PCR for geometric random graphs under selective node removal attacks, that is, the fraction of nodes that can be selectively removed without letting the PCR below a certain threshold (i.e., α). The results are similar to those illustrated in Fig. 5.10 and they are compared in Fig. 5.17. First, when the original APC is large, the network is more robust to random node removal attacks than to selective node removal attacks. For example, for α being 95% and the original APC being 12, when nodes are removed randomly, p can be 0.6, while under selective node removal attacks, p is 0.5. This indicates that selective node removal can cause more damage than random node removal when the original network density is high. Second, it surprising to see that when the original APC is relatively small and the PCR requirement is high, random node removal can cause even more damage than selective node removal attacks.

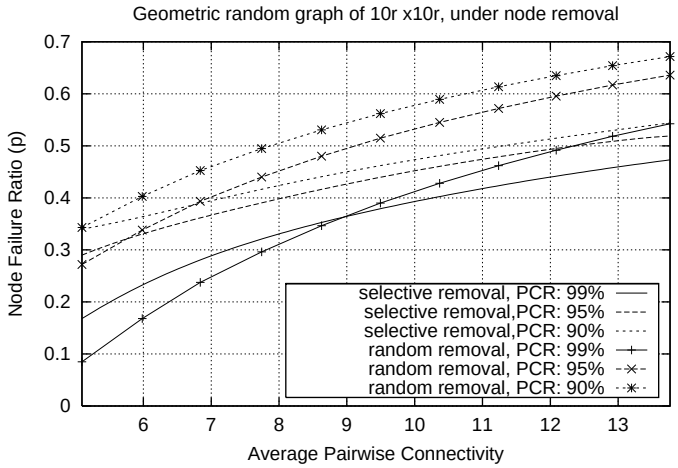

Figure 5.17: Comparison of α-p-resilience in PCR for geometric random graphs between random failure and selective attack

For example, for α being 99% and the original APC being 5, p is 18% under selective node removal, while p is 9% under random node removal. This can be explained as follows: when nodes are removed in decreasing order of degrees, those nodes being first removed are usually in areas with higher node density, and removal of such nodes may cause less effect on node isolation or network disconnection comparing to removal of nodes from low density area. This is why there is less effect on PCR.

Fig. 5.18 demonstrates the comparisons under different node removal patterns in geometric random graphs. In these comparisons, three node densities are studied: 5, 10, 15. Fig. 5.18(a) shows the comparison results with the original node density being 5. From this set of comparisons we can see that when the node removal ratio is larger than 10%, selective node removal attacks may cause more damage than partition attacks. This makes sense, since under low node density and with a considerable amount of selective node removal, the network will be partitioned into many small disconnected pieces, while partition attacks give rise to larger connected subsets. Further, from this set of comparisons we can also see

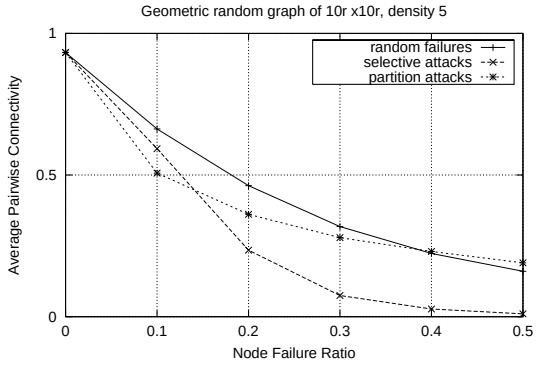

(a)

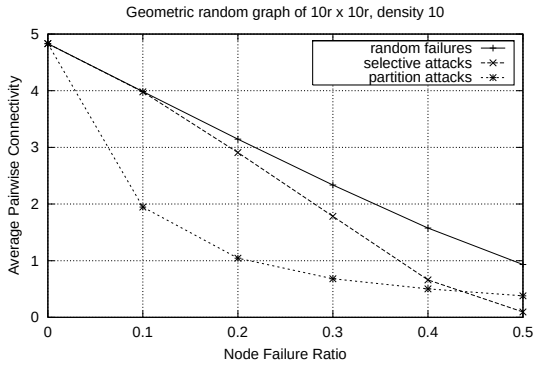

(b)

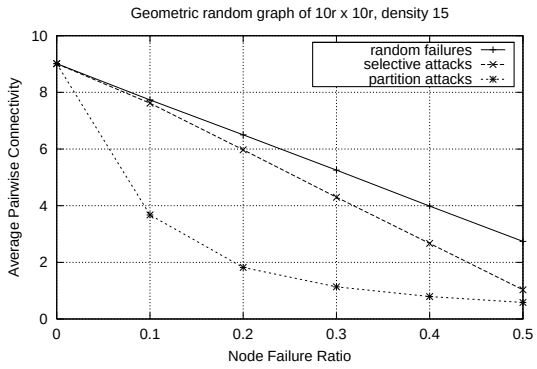

(c)

Figure 5.18: Comparison of APC under different attacks in geometric random graphs

that when the node removal percentage is more than 40%, the APC corresponding to partition attacks is actually higher than the APC corresponding to random node failure.

Fig. 5.18(b) and Fig. 5.18(c) show the comparison results for node densities 10 and 15. From these comparisons we can see that with the increase of node density, the effects of partition attacks become more and more severe. For example, when the original node density is 10, in only one situation (i.e., node failure ratio 50%) partition attack can cause more damage than selective attack, while when node density is 15, in no situations does selective attack perform better than partition attack from the attackers' point of view. Thus, partition attacks can cause more damage than selective node removal attacks when the network node density is high.

We have also compared the evolution of pairwise connectivity ratio (PCR) under different node removal patterns, with the results being illustrated in Fig. 5.19. First we examine the comparison under node density 5. Similar to the case of Fig. 5.18(a), selective attacks can cause more damage than partition attacks when the node failure ratio is larger than 20%, which has been explained before. One very interesting observation from Fig. 5.19(a) is that PCR under selective attacks is even a little bit higher than PCR under random node removal when the node failure ratio is 10%. This can be explained as follows. For geometric random graphs, selective node removal according to degree distribution tends to remove nodes in denser regions. Since the regions are denser it is less likely that this will cause a neighbor to become isolated. Another interesting observation is that although the APC under selective attack is lower than the APC under partition attack when the node failure ratio is 20% (shown in Fig. 5.18(a)), the PCR is still a little bit higher (shown in Fig. 5.19(a)). This observation implies that under some attacks

a higher APC may not indicate a higher PCR.

The comparison of PCR under various attacks for node densities 10 and 15 have also been illustrated in Fig. 5.19. From the comparisons presented in Fig. 5.19(b) and Fig. 5.19(c) we can see that when the node density is high, partition attacks become very severe in degrading the pairwise connectivity ratio, which is also consistent with the results presented in Fig. 5.18(b) and Fig. 5.18(c). Further, when the node density is very high (e.g., 15), even selective attacks can cause almost no degradation to the pairwise connectivity ratio. In other words, selective attack is not an effective attacking strategy when the node density is high.

5.5 Summary

In this chapter, we have studied the service availability of wireless ad hoc networks based on average pairwise connectivity and pairwise connected ratio, and derived theoretical upper-bound for the average pairwise connectivity which can approximate the exact value very well. Based on the proposed metric, α-p-resilience, we have also studied the fault tolerance and attack resilience of wireless ad hoc networks under different node failure patterns: random node removal, selective node removal, and partition attack. Experimental studies have demonstrated that when the node density is relatively high, wireless ad hoc networks are more sensitive to partition attacks than selective node removal attacks and random node failures, and selective node removal attacks are a little bit more damaging than random node removal; when the node density is extremely low, all the three node removal methods have similar effects, with partition attacks and selective node removal attacks being a little bit more damaging than random node removal.

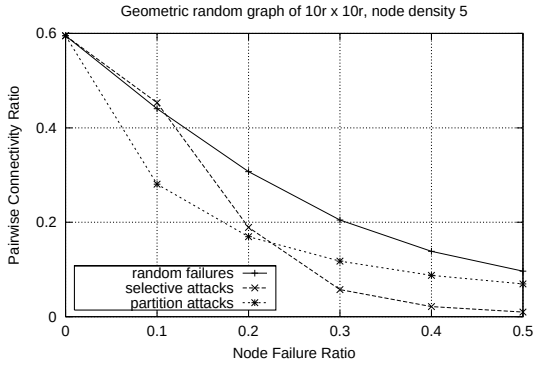

(a)

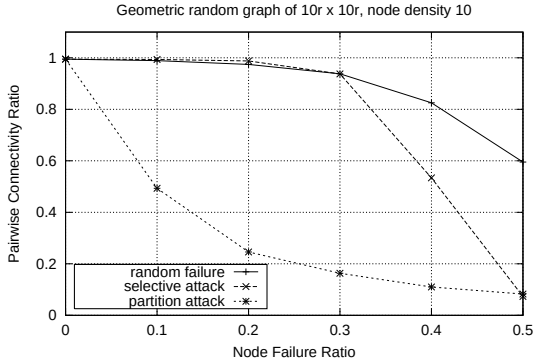

(b)

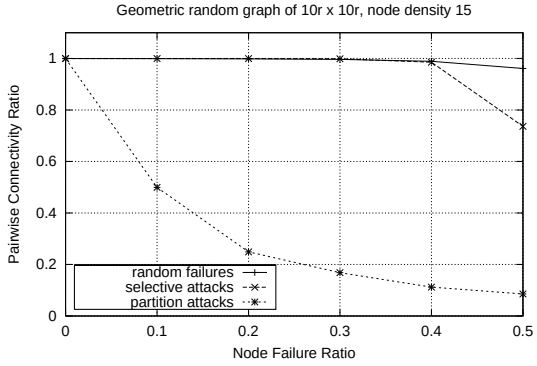

(c)

Figure 5.19: Comparison of PCR under different attacks in geometric random graphs

Chapter 6

Conclusions and Future Work

6.1 Conclusion

In this dissertation we have made important progress on the following two important issues: lifetime maximization in randomly deployed wireless sensor networks and fault tolerance and attack resilience measurement in wireless ad hoc networks.

In the first part of this dissertation we have studied how to maximize the network lifetime of randomly deployed wireless sensor networks by applying adaptive traffic distribution and power control scheme. After abstracting the network into layers, we are able to model the optimization problem as linear program. We first studied a simple scenario where only transmission power consumption was considered. The numerical results show that in order to maximally extend the network lifetime, each node should split its traffic into two portions with one portion is sent directly to the sink and the other one to its neighbor in the next inner layer. Then we proved that this is generally true and the optimal solution is unique. We then generalized the model by incorporating processing and receiving energy consumption. In this case, similar results have also been observed: for each packet to be

sent, the sender should either transmit it using the transmission range with the highest energy efficiency per bit per meter, or transmit it directly to the sink. We then proposed a fully distributed algorithm to adaptively split traffic and adjust transmission power for randomly deployed wireless sensor networks. Extensive simulation studies have also confirmed that the network lifetime can be dramatically extended by applying the proposed approach in various scenarios.

Besides studying lifetime maximization in fully deployed sensor networks, in this dissertation we have also investigated how to further extend the lifetime of wireless sensor networks via joint relay deployment and adaptive traffic distribution. In this case, after a sensor network has been randomly deployed, some extra relay nodes will be put into the network in a partially controlled way such that the network lifetime can be maximally extended. Since this is a mixed-integer nonlinear programming problem, which is generally NP-hard, we proposed a greedy heuristic to attack it. Our studies show that if the relay nodes can be deployed in a right way, significant network lifetime extension can be achieved even with a small portion of extra relay nodes.

In the second part of this dissertation we have investigated how to effectively measure the fault tolerance and attack resilience of randomly deployed wireless ad hoc networks. We first introduced two metrics to measure the service quality of such networks: average pairwise connectivity and pairwise connected ratio, where the former denotes the average number of node-disjoint paths per node pair in a network and the latter is the fraction of node pairs that are pairwise connected. Based on these two metrics, we came out the fault tolerance and attack resilience metric: α-p-resilience, where a network is α-p-resilient if at least α portion of nodes pairs remain connected as long as no more than p fraction of nodes are removed

from the network. Under the new measurement metric, we then studied the fault tolerance and attack resilience of wireless ad hoc networks under different node failure patterns, specifically random node removal, selective node removal, and partition attack.

6.2 Future Work

Although some progress has been made in this dissertation, there are still many other important issues left unsolved. Next we discuss some interesting and important topics that are related to our research.

One interesting topic is network lifetime maximization via joint in-network data aggregation and adaptive traffic distribution. As demonstrated in [9, 17, 29, 32, 36], in-network data aggregation is able to significantly extend the network lifetime by decreasing the forwarding burden in wireless sensor networks. However, data aggregation can be computation intensive and energy consuming. If in-network data aggregation is not designed properly, those nodes that are responsible to perform data aggregation will die much faster than others. However, this situation can be alleviated by letting such nodes forward fewer packets, which can be realized by joint consideration of in-network data aggregation and adaptive traffic distribution. Motivated by this idea, in the future we would like to study how to jointly perform in-network data aggregation and adaptive traffic distribution and power control to maximize the network lifetime.

Another interesting topic is to study the effect of different network lifetime definitions on the solution of lifetime maximization problem under resource constraint. In this dissertation, we define *network lifetime* as the time elapsing between network deployment and the moment when the first node dies. However, this def-

inition may not always be the most meaningful one. For example, in order for a sensor network to function properly, it has to maintain a certain coverage, therefore in such situation one alternative lifetime definition can be the time elapsing between network deployment and the moment when the network losses its required coverage. Then the question is: Are the solutions derived from previous lifetime definition also optimal under new definitions? Our analysis indicates that although in some situations they are, in most situations they are not. Then if they are not optimal, how far are they away from the optimal solution? Studying and comparing the optimal solutions derived under different lifetime definitions can be an interesting topic, which can help us better understand the problem and may lead us to solutions for more general setting.

BIBLIOGRAPHY

[1] I. Akyildiz, W. Su, Y. Sankarasubramaniam, and E. Cayirci. A survey on sensor networks. *IEEE Communication Magazine*, 40(8):102–114, 2002.

[2] R. Albert, H. Jeong, and A.-L. Barabási. Error and attack tolerance of complex networks. *Nature*, 406:378–382, 2000.

[3] S. Bandyopadhyay and E. J. Coyle. An energy efficient hierarchical clustering algorithm for wireless sensor networks. In *IEEE INFOCOM*, pages 1713–1723, 2003.

[4] C. Bettstetter. On the minimum node degree and connectivity of a wireless multihop network. In *MOBIHOC*, 2002.

[5] M. Bhardwaj and A. P. Chandrakasan. Bounding the lifetime of sensor networks via optimal role assignments. In *IEEE INFOCOM*, March 2002.

[6] B. Bollóbas. *Modern Graph Theory*. Springer, 1998.

[7] B. Bollóbas. *Random Graphs*. Academic Press, 2nd edition, 2001.

[8] A. Boukerche, X. Cheng, and J. Linus. Energy-aware data-centric routing in microsensor networks. In *ACM MSWiM*, pages 42–49, 2003.

[9] A. Boulis, S. Ganeriwal, and M.B. Srivastava. Aggregation in sensor networks: An energy-accuracy trade-off,. In *Sensor Network Protocols and Applications (SNPA)*, 2003.

[10] A. Broder, R. Kumar, F. Maghoul, P. Raghavan, S. Rajagopalan, R. Stata, A. Tomkins, and J. Wiener. Graph structure in the web. *Computer Networks*, 33:309–320, 2000.

[11] Q. Cao, T. Abdelzaher, T. He, and J. Stankovic. Towards optimal sleep scheduling in sensor networks for rare-event detection. In *International Conference on Information Processing in Sensor Networks (IPSN)*, April 2005.

[12] A. Cerpa, J. Elson, D. Estrin, L. Girod, M. Hamilton, and J. Zhao. Habitat monitoring: Application driver for wireless communications technology. In *ACM SIGCOMM Workshop on Data Communications in Latin America and the Caribbean*, April 2001.

[13] J.-H. Chang and L. Tassiulas. Energy conserving routing in wireless ad-hoc networks. In *IEEE INFOCOM*, 2000.

[14] I. Chlamtac and A. Faragó. A new approach to the design and analysis of peer-to-peer mobile networks. *ACM/Baltzer Wireless Networks*, 5, Aug 1999.

[15] R. Cohen, K. Erez, D. ben Avraham, and S. Havlin. Resilience of the internet to random breakdowns. *Phys. Rev. Lett.*, 85:4626–4628, 2000.

[16] R. Cohen, K. Erez, D. ben Avraham, and S. Havlin. Breakdown of the internet under intentional attack. *Phys. Rev. Lett.*, 86:3682–3685, 2001.

[17] R. Cristescu, B. Beferull-Lozano, and M. Vetterli. On network correlated data gathering. In *IEEE INFOCOM*, March 2004.

[18] J. A. Dunne, R. J. Williams, and N. D. Martinez. Food-webstructure and network theory: The role of connectance and size. In *Proc. Natl. Acad. Sci. USA*, volume 99, pages 12917–12922, 2002.

[19] J. A. Dunne, R. J. Williams, and N. D. Martinez. Network structure and biodiversity loss in food webs: Robustness increases with connectance. *Ecology Lett.*, 5:558–567, 2002.

[20] C. Efthymiou, S. Nikoletseas, and J. D.P. Rolim. Energy balanced data propagation in wireless sensor networks. In *4th Workshop on Algorithms for Wireless, Mobile, Ad Hoc and Sensor Networks*, 2004.

[21] P. Erdös and A. Rényi. On random graphs. *Publ. Math. Debrecen*, 6:290–297, 1959.

[22] P. Erdös and A. Rényi. On the evolution of random graphs. *Publ. Math. Inst. Hungar. Acad. Sci.*, 5:17–61, 1960.

[23] D. Estrin, L. Girod, G. Pottie, and M. Srivastava. Instrumenting the world with wireless sensor networks. In *International Conference on Acoustics, Speech, and Signal Processing (ICASSP '01)*, May 2001.

[24] W. R. Heinzelman, A. Chandrakasan, and H. Balakrishnan. Energy-efficient communication protocol for wireless microsensor networks. In *IEEE Hawaii International Conference on System Sciences*, 2000.

[25] P. Holme, B. J. Kim, C. N. Yoon, and S. K. Han. Attack vulnerability of complex networks. *Phys. Rev. E*, 65(056109), 2002.

[26] Y. T. Hou, Y. Shi, H. D. Sherali, and S. F. Midkiff. Prolonging sensor network lifetime with energy provisioning and relay node placement. In *IEEE SECON*, Sep. 2005.

[27] Y. T. Hou, Y. Shi, H. D. Sherali, and S. F. Midkiff. Prolonging sensor network lifetime with energy provisioning and relay node placement. In *IEEE SECON*, September 2005.

[28] P.-H. Hsiao, A. Hwang, H. T. Kung, and D. Vlah. Load-balancing routing for wireless access networks. In *IEEE INFOCOM*, pages 986–995, 2001.

[29] C. Intanagonwiwat, R. Govindan, and D. Estrin. Directed diffusion: A scalable and robust communication paradigm for sensor networks. In *MOBICOM*, August 2000.

[30] H. Jeong, S. Mason, A.-L. Barabási, and Z. N. Oltvai. Lethality and centrality in protein networks. *Nature*, 411:41–42, 2001.

[31] O. Kallenberg. *Foundations of Modern Probability.* New York: Springer-Verlag, 1977.

[32] B. Krishnamachari, D. Estrin, and S. Wicker. Modelling data-centric routing in wireless sensor networks. In *IEEE INFOCOM*, 2002.

[33] J. Lee, B. Krishnamachari, and C.C. J. Kuo. Impact of heterogeneous deployment on lifetime sensing coverage in sensor networks. In *IEEE SECON*, October 2004.

[34] P. Leone, S. Nikoletseas, and J. D. P. Rolim. An adaptive blind algorithm for energy balanced data propagation in wireless sensor networks. In *Proceedings of the First International Conference (DCOSS)*, pages 35–48, 2005.

[35] X. Li, P. Wan, Y. Wang, and C. Yi. Fault tolerant deployment and topology control in wireless networks. In *MOBIHOC*, Annapolis, MD, June 2003.

[36] M. Lotfinezhad and B. Liang. Effect of partially correlated data on clustering in wireless sensor networks. In *IEEE SECON*, October 2004.

[37] Matt Loy, editor. *Understanding and Enhancing Sensitivity in Receivers for Wireless Applications*. Texas Instruments, Technical Brief SWRA030, 1999.

[38] J. Luo and J.-P. Hubaux. Joint mobility and routing for lifetime elongation in wireless sensor networks. In *IEEE INFOCOM*, 2005.

[39] W. Manges. It's time for sensors to go wireless. part 1: Technological underpinnings. *Sensors Magazine*, April 1999.

[40] W. Manges. It's time for sensors to go wireless. part 2: Take a good technology and make it an economic success. *Sensors Magazine*, May 1999.

[41] S. Meguerdichian, F. Koushanfar, M. Potkonjak, and M.B. Srivastava. Coverage problems in wireless ad-hoc sensor networks. In *IEEE Infocom*, volume 3, pages 1380–1387, April 2001.

[42] V. P. Mhatre, C. Rosenberg, D. Kofman, R. Mazumdar, and N. Shroff. A minimum cost heterogenous sensor network with a lifetime constraint. *IEEE Transactions on Mobile Computing*, 4(1), January/February 2005.

[43] W. Najjar and J.-L. Gaudiot. Network resilience: A measure of network fault tolerance. *IEEE Transactions on Computers*, 39(2):174–181, February 1990.

[44] M. E. J. Newman. The structure and function of complex networks. *SIAM Review*, 45(2):167–256, 2003.

[45] M. E. J. Newman, S. Forrest, and J. Balthrop. Email networks and the spread of computer viruses. *Phys. Rev. E*, 66(035101), 2002.

[46] M. D. Penrose. On k-connectivity for a geometric random graph. *Wiley Random Structures and Algorithms*, 15(2):145–164, 1999.

[47] C. Perkins. *Ad Hoc Networking*. Addison-Wesley, 2000.

[48] G.J. Pottie and W.J. Kaiser. Wireless integrated network sensors. *Communications of the ACM*, 43(5):51–58, May 2000.

[49] O. Powell, P. Leone, and J. Rolim. Energy optimal data propagation in wireless sensor networks. Technical report, arXiv.org automated e-print archives, Report CS-0508052, 2005.

[50] D. Pradhan. Dynamically restructurable fault-tolerant processor network architectures. *IEEE Transactions on Computers*, C-34:434–447, May 1985.

[51] V. Rajendran, K. Obraczka, and J. Garcia-Luna-Aceves. Energy-efficient, collision-free medium access control for wireless sensor networks. In *ACM Sensys*, 2003.

[52] R. C. Shah and J. M. Rabaey. Energy aware routing for low energy ad hoc sensor networks. In *IEEE Wireless Communications and Networking Conference*, pages 350–355, 2002.

[53] S. Singh, M. Woo, and C. S. Raghavendra. Power aware routing in mobile ad hoc networks. In *ACM MobiCom*, pages 181–190, 1998.

[54] S. Singh, M. Woo, and C. S. Raghavendra. Maximum battery life routing to support ubiquitous mobile computing in wireless ad hoc networks. *IEEE Communications Magazine*, pages 138–147, 2001.

[55] R. Solomonoff and A. Rapoport. Connectivity of random nets. *Bull. Math. Biophys.*, 13:107–117, 1951.

[56] F. Sun and M. Shayman. Lifetime maximizing adaptive power control in wireless sensor networks. Technical report, University of Maryland, The Institute for Systems Research, 2006.

[57] F. Sun and M. Shayman. Lifetime maximizing adaptive traffic distribution and power control in wireless sensor networks. Technical report, University of Maryland, The Institute for Systems Research, 2006.

[58] F. Sun and M. Shayman. Prolonging network lifetime via partially controlled node deployment and adaptive data propagation in wsn. In *Conference on Information Sciences and Systems*, March 2007.

[59] F. Sun and M. Shayman. On pairwise connectivity of wireless multihop networks. *International Journal of Security and Networks*, to appear.

[60] C. K. Toh. *Ad Hoc Mobile Wireless Networks: Protocols and Systems*. Prentice Hall PTR, 2001.

[61] M. Tubaishat and S. Madria. Sensor networks: an overview. *IEEE Potentials*, 22(2):20–23, April 2003.

[62] S. Vasudevan, C. Zhang, D. Goeckel, and D. Towsley. Optimal power allocation in wireless networks with transmitter-receiver power tradeoffs. In *IEEE INFOCOM*, April 2006.

[63] J. Wang and I. Howitt. Optimal traffic distribution in minimum energy wireless sensor networks. In *Globecom*, 2005.

[64] Y. Xin, T. Guven, and M.A. Shayman. Relay deployment and power control for lifetime elongation in sensor networks. In *IEEE ICC*, June 2006.

[65] N. Xu, S. Rangwala, K. Chintalapudi, D. Ganesan, A. Broad, R. Govindan, and D. Estrin. A wireless sensor network for structural monitoring. In *ACM Sensys*, November 2004.

[66] W. Ye, J. Heidemann, and D. Estrin. Medium access control with coordinated adaptive sleeping for wireless sensor networks. *IEEE/ACM Transactions on Networking*, 12(3):493–506, 2004.

[67] O. Younis and S. Fahmy. Distributed clustering in ad-hoc sensor networks: A hybrid, energy-efficient approach. In *IEEE INFOCOM*, 2004.

[68] W. Yu and K. J. R. Liu. Attack-Resistant Cooperation Stimulation in Autonomous Ad Hoc Networks. *To appear in IEEE Journal on Selected Areas in Communications: Autonomic Communication Systems*, 2005.

[69] H. Zhang and J. C. Hou. On the upper bound of a-lifetime for large sensor networks. *ACM Transactions on Sensor Networks*, 1(2):272–300, November 2005.